Combining Magnetic Resonance Imaging and Electroencephalography in the Investigation of Interictal Epileptic Spikes

Christian-George Bénar

Department of Biomedical Engineering
McGill University, Montréal, Canada

August 2004

A thesis submitted to the Faculty of Graduate Studies and Research in fulfillment of the requirements for the degree of Ph.D. in Biomedical Engineering.

2004/08/27

A mon père, Georges Benayoun Bénar

(Tlemcen, 26 février 1926 - Cannes, 14 juillet 2000)

"Il faut toujours voir à la fois dans l'espace et dans le temps"

Abstract

Interictal spikes are spontaneous neuronal discharges that occur between epileptic seizures, and that constitute a specific marker of epilepsy. The topic of our doctoral research is to localize in a noninvasive manner the regions of the brain responsible for generating the spikes. Such information is of great interest in the presurgical evaluation for pharmacoresistant epilepsy.

In this context, we have studied the possibility of using a combination of two techniques, namely electroencephalography (EEG) and magnetic resonance imaging (MRI). Specifically, we have investigated three tracks for the combination of EEG and MRI.

First, anatomical information from MRI can be used for improving EEG source localization. Our example is the modelling of postsurgical brain and skull defects, which affect the conductive properties of the head.

Second, the EEG can be recorded inside the MR scanner and thereby allows the investigation of spontaneous epileptic spikes with functional MRI (fMRI). We evaluated the quality of EEG within the scanner, and measured the spatial and temporal fMRI response to spikes.

Third, the information from the two modalities can be combined in order to benefit from both the good spatial resolution of fMRI and the excellent temporal resolution of EEG. We have proposed to build statistical maps for EEG source localization in order to identify common areas of activation in EEG and fMRI.

Résumé

Les pointes épileptiques sont des décharges neuronales qui surviennent entre les crises épileptiques et qui constituent un marqueur spécifique de l'épilepsie. Le sujet de notre recherche doctorale est de localiser de façon non-invasive les régions du cerveau où sont générées les pointes. Ce type d'information s'avère très utile lors de l'évaluation pré-chirurgicale des patients atteints d'épilepsie pharmaco-résistante.

Dans ce contexte, nous avons étudié la possibilité d'utiliser une combinaison de deux techniques: l'électroencéphalographie (EEG) et l'imagerie par résonance magnétique (IRM). Plus spécifiquement, nous avons examiné trois possibilités pour combiner l'EEG et l'IRM.

Premièrement, il est possible d'utiliser l'information anatomique provenant de l'IRM pour améliorer la localisation de sources en EEG. Nous avons choisi d'étudier et de modéliser les défauts du cerveau et du crâne qui découlent de la chirurgie de l'épilepsie, et qui modifient les propriétés conductrices de la tête.

Deuxièmement, l'EEG peut être enregistré à l'intérieur de l'imageur IRM, ce qui permet d'examiner les pointes épileptiques à l'aide de l'IRM fonctionnelle (IRMf). Nous avons évalué la qualité de l'EEG dans le scanner, et nous avons mesuré les réponses spatiale et temporelle aux pointes enregistrées par l'IRMf .

Troisièmement, les informations provenant des deux modalités peuvent être combinées pour profiter la fois de la bonne résolution spatiale de l'IRMf et de l'excellente résolution temporelle de l'EEG. Nous avons proposé de construire des cartes statistiques pour la localisation de sources en EEG, ce qui permet d'identifier les régions activées de concert en EEG et en IRMf.

Acknowledgments

This thesis was made possible thanks to the support of a Master studentship of the Natural Sciences and Engineering Research Council of Canada (NSERC), a doctoral studentship from the Canadian Institutes of Health Research (CIHR), as well as the CIHR grant MOP-38079.

I would like to thank warmly Jean Gotman for his impeccable supervision, his constant support and relevant advice. I am very grateful to my Ph. D. committee, Francois Dubeau, Michael Guevara, Robert Kearney, Bruce Pike for their regular guidance and useful comments. I thank Pina Sorrini and Toula Papadopoulos for their kind help in administrative issues.

Thanks also to Lorraine Allard, Nicole Drouin and all the technicians and staff of the EEG department, that have always been there to give me access to data and support in all practical aspects of EEG, to André Cormier and the fMRI technicians, and to Anne Alex and Colin Hawco for their contribution to the EEG-fMRI recording sessions.

Many thanks to all the persons that I collaborated with, and to those who helped me gathering data, Josée Allard for EEG recording support, André Leduc for the conductivity measurements, Aviva Abosh for taking me into the OR, and Lahbib Soualmi for the depth EEG electrode positions.

Thanks also to the researchers, fellows and students for giving me precious help and for sharing ideas over the years: Neda Bernasconi-Ladbon and Andrea Bernasconi in imaging epilepsy, Roger Gunn in statistics, Louis Collins in image processing, Chris James in Matlab and Independent Component Analysis, Isabelle Merlet and Michael Scherg in dipole modelling, Keith Worsley and Jean-Baptiste Poline in statistical modelling, Yunhua Wang, Sylvain Baillet, Benoît Champagne and Sunil Kukreja in array processing, Christophe Grova in statistical issues and handling LaTeX, Don Gross, Abdullah Al-Asmi, Yahya Agha Khani and Eliane Kobayashi in epilepsy and clinical interpretations, Bojana Stefanovic for fMRI protocols, Andrew Bagshaw in fMRI considerations and for proof-reading this manuscript. I am indebted to Andrew, Eliane, Christophe and Jean Daunizeau for useful suggestions on the manuscript.

Thanks to Valentina Petre and Michael Ferreira for support in fMRI acquisition and data processing, to Jean-Francois Malouin and Peter Neelin for support on the computers

of the Brain Imaging Center. Thanks to Michael Wagner for support on Curry software.

I must acknowledge also the other students for maintaining a friendly atmosphere - I am thinking for example of David Grennan and Marc Saab - and to the musicians at the MNI for the great time (thanks to Ernst Meyer and his contagious enthusiasm!).

Merci à toi Julie pour ta patience et pour tout le reste, et à toi Pierrot pour ton amitié et pour m'avoir montré quelques voies. Merci à ma mère pour m'avoir transmis le goût des voyages et de la découverte...

Contribution of Authors

Article 1: Modelling of Post-surgical Brain and Skull Defects in the EEG Inverse Problem with the Boundary Element Method

Authors: Christian-G. Bénar and Jean Gotman.

I conducted all the experiments and wrote the draft of the manuscript.

Jean Gotman supervised the project. He helped me in the design of experiments and in the writing of the manuscript.

Article 2: Quality of EEG in Simultaneous EEG-fMRI for Epilepsy

Authors: Christian-G. Bénar, Yahya Aghakhani, Yunhua Wang, Aaron Izenberg, Abdullah Al-Asmi, François Dubeau, Jean Gotman.

I designed the methods for filtering the artefacts, implemented and tested them with the Matlab software. I performed statistical analysis on the results of the EEG reviews by Y.A. and A.I. I wrote the methods, results and parts of the discussion sections of the manuscript.

Yahya Agha-Khani reviewed the EEG in the series of patients for marking the spikes, and assessing the quality of the filters. He gathered the clinical data for the patients.

Yunhua Wang had the idea of the PCA filter and made the initial tests of PCA filtering. He participated in the development of the EEG-fMRI recording protocol.

Aaron Izenberg reviewed the EEG in the series of patients for testing the impact of PCA and ICA filters.

Abdullah Al-Asmi participated in the development of the EEG-fMRI recording protocol.

François Dubeau referred the patients, making sure they fulfilled all criteria, and participated in improving the manuscript.

Jean Gotman supervised the project. He wrote the introduction of the manuscript and parts of the discussion.

Article 3: The BOLD Response to Interictal Epileptiform Discharges

Authors: Christian-G. Bénar, Donald W. Gross, Yunhua Wang, Valentina Petre, Bruce Pike, François Dubeau, Jean Gotman.

I had the idea of measuring the temporal response to the spikes and the correlation between EEG and fMRI signals. I performed all data analysis, and wrote the draft of the manuscript.

Don W. Gross was part of the initial development of the EEG-fMRI technique at the MNI, in terms of recording set-up, patient selection and interpretation of the results.

Yunhua Wang participated in the development of the EEG-fMRI recording protocol.

Valentina Petre and Bruce Pike designed the fMRI acquisition scheme. In particular, V. Petre designed the fMRI analysis protocol and conducted the initial tests on the quality of fMRI images.

François Dubeau referred the patients, making sure they fulfilled all criteria, and participated in improving the manuscript

Jean Gotman supervised the project and participated in the writing of the manuscript.

Article 4: Statistical Maps for EEG Dipolar Source Localization

Authors: Christian-G. Bénar, Roger N. Gunn, Christophe Grova, Benoît Champagne, Jean Gotman.

I had the original idea of the guidelines of the method. I implemented and tested the algorithm, created the simulated data and performed data analysis. I wrote the draft of the manuscript.

Roger Gunn helped me implementing the method within a statistical framework.

Christophe Grova suggested the bootstrap method and helped me implementing it. He participated in the revision of the manuscript.

Benoît Champagne participated in the design and implementation of the method, in particular in terms of numerical issues.

Jean Gotman supervised the project and participated in the writing of the manuscript.

Statement of Originality

To the best of our knowledge:

• Our study on the modelling of postsurgical defects (chapter 5) was the first to present and evaluate modelling of skull holes and cavities with the boundary element method (BEM). Previous studies of such effects were conducted with the finite element or finite differences methods. We were also the first to investigate the conductivity and effect of the methacrylate plugs used to fill the surgical holes.

• Our study of the quality of EEG (chapter 6) was the first to quantify on a group of subjects the effect of recording procedures and filtering techniques on the quality and readability of EEG in simultaneous EEG-fMRI for epilepsy. Previous reports consisted in visual assessments of the EEG only [Lemieux 01b, Baudewig 01]. We reported for the first time the use of ICA (independent component analysis) in this context.

• The study on the BOLD fMRI response to epileptic spikes (chapter 7) was the first to present a series of patients, as well as differences in responses across patients and across regions in EEG-fMRI for epilepsy. A previous report had been made of the response in one region for one patient [Lemieux 01b]. We have also presented the only attempt to correlate the amplitude of the BOLD response to that of the spikes.

• The technique we have presented for establishing statistical maps in EEG was the first to compute such maps in the context of dipolar source localization. We have also established a method for computing a threshold of significance for a given solution. Previous studies were in the context of distributed sources [Dale 00], cortical patches [Schmidt 99] or beamformer [Barnes 03].

Contents

List of Figures

List of Tables

Chapter 1

Introduction

Epilepsy[1] is a common neurological disorder, which affects of the order of 1 % of the population in industrialized countries (around 300 000 persons in Canada) and even more in less developed countries. It is characterized by recurrent epileptic seizures, which are sudden excessive discharges of brain cells. Many factors can produce the epileptic state, for example head injuries, vascular damages, tumours or genetic factors; it is in fact more proper to make reference to *the epilepsies*. Seizures are classified into *partial* (focal or local), which start in a limited part of the brain, and *generalized*, where most of the brain is involved from the onset.

In most patients, epilepsy can be treated with medication that typically aims at reducing the neuronal excitability, with efficiency depending on the type and causes of epilepsy. However, medication is inefficient in approximately 20 % of the patients: these patients are said to have refractory or "pharmacoresistant" epilepsy.

When epilepsy is focal, i.e. when seizures start in a very limited part of the brain[2], a surgical procedure can be considered in order to remove the part of the brain responsible for the seizures. This removal (resection) of a part of the brain may appear like a drastic option, but one has to consider the severe handicap that arises from the epileptic condition. Also, an effort is made to avoid resecting regions that would lead to too severe post-surgical losses. Moreover, the resected region is often damaged, and the brain may have already compensated by involving other areas.

[1] From Greek *epilepsia*, from *epi*, on, and *lambanein*, to seize.

[2] Often referred to as the "epileptic focus". As this is not a simply defined notion - cf. 2.3.2 - this name has been discouraged.

Presurgical evaluation consists in combining many sources of information on the patient's epilepsy in order to define as precisely as possible the zone to be removed. These techniques can be referred to as either *non-invasive*, i.e. with minimal physical interference with the patient, or *invasive*, for example when electrodes are actually placed within the brain (depth electrodes).

The topic of this doctoral research is the combination of two non-invasive techniques for presurgical evaluation, namely electroencephalography (EEG) and magnetic resonance imaging (MRI).

On the one hand, the EEG is a recording of the electrical potentials at the surface of the head that can be used to infer the location of the brain sources producing the epileptic discharge. However, EEG localization is limited as it is trying to infer electromagnetic sources within a volume given measurement at the surface only. On the other hand, MRI enables measurements directly within the head. It can be used to produce anatomical images of the brain with a very fine spatial resolution. It can also be used to monitor the activity of the brain; this is the functional MRI (fMRI). In the last decade, there has been an explosion of fMRI studies aiming at mapping the functions of the brain.

There are several reasons for using EEG and MRI in combination for the study of epilepsy. First, MRI can provide anatomical information in order to improve localization based on EEG. Second, the recent possibility of recording EEG within an MRI scanner allows the study of epileptic discharges with fMRI. Third, the EEG can bring fine temporal information to complement the mainly spatial results of fMRI.

In chapters 2 to 4, we will provide background information on presurgical evaluation, EEG source localization and functional MRI respectively. Then, we will present our results on the combined use of EEG and fMRI in the form of scientific articles (chapters 5 to 8). Finally, we will conclude and present possible new lines of research in chapter 9.

Chapter 2

Presurgical Evaluation of Epilepsy

The goal of presurgical evaluation is to gain information on the zone of the brain that can be resected in order to render the patient seizure-free. Considerable knowledge has been accumulated on patterns of interictal spiking and of ictal onset and propagation, which can be related to the clinical manifestations. This is complemented by a whole spectrum of techniques, from magnetic resonance to neuropsychology tests.

2.1 A brief History of Epilepsy Investigation

(This section is based on [Rosenow 01], [Goldenson 97], [Wolf 91], and [Flanigin 91]).

The beginnings of modern epilepsy investigation took place in the second half of the nineteenth century. The most prominent figure of that time was probably John Hughlings Jackson (Green Hammerton, Yorkshire 1835 - London 1911), a neurologist at the London Hospital and the National Hospital, Queen Square. He pointed out the major role of the cerebral cortex, and defined epilepsy as "occasional, sudden, excessive, rapid and local discharges of grey matter" [Jackson 73]. He also gave in 1870 a classification of seizures into generalized ("Those in which the spasm affects both sides of the body almost contemporaneously") and partial ("Those in which the fit begins by deliberate spasm on one side of the body, and in which parts of the body are affected one after another") [Jackson 70]. These ideas were those of a pioneer, and are still in use today. They were based mainly on the observation of the clinical manifestations, for example convulsions that would start in the hand and propagate along the arm (the "Jacksonian march"). In some cases, confirmation

was brought by the autopsy of epileptic patients, where brain lesions could be observed directly. From the start, the localization of functions into separate brain areas and the comprehension of epilepsy were helping one another - Wilder Penfield would say later that epilepsy is a "window on the brain".

The conclusions of Jackson were confirmed by experimenters who worked on animals, such as Gustav Theodor Fritsch and Eduard Hitzig on dogs in 1870 and David Ferrier on monkeys in 1873. For example, Fritsch and Hitzig showed that electrical stimulation of the dog's frontal cortex caused movement of the body on the opposite side.

The work of J. H. Jackson, and of others such as Ferrier and Gowers, opened the way to modern epilepsy surgery. The approach of the time consisted in localizing the region responsible for the seizures by observing the clinical signs, and then operating in order to remove the lesion. For example, according to Gowers, trephination is possible when "the local commencement of the fits suggests that the disease causing them is at the surface of the brain, involving the motor convolutions which are adjacent to the fissure of Rolando" [Gowers 85].

The first successful operation performed on the basis of seizure symptomatology only was by William Macewen in 1879. The leading figure of the time was however Victor Horsley (London 1857 - Amara 1916), who performed a series of surgeries starting in 1886, working in conjunction with Ferrier and Jackson.

The pioneers of electrical stimulation of the exposed cortex under local anaesthesia were German: Fedor Krause in Berlin and Otfrid Foerster in Breslau. Electrical stimulation helped both in localizing an assumed epileptic focus, i.e. the region where stimulation would reproduce the clinical symptoms, but also in avoiding the removal of important parts of the motor cortex. Foerster operated patients with epilepsy secondary to war wounds, and initiated a collaboration with Wilder Penfield in 1928. In 1932, Krause and Schum in Berlin published a monograph where they advocated the use of surgery - even when no visible lesion was present - in order to remove the focus or "primary convulsive center" [Krause 32].

A great step forward occurred with the discovery of the human electroencephalogram (EEG) by the German psychiatrist Hans Berger (Neuses 1873 - Jena 1941) (see section 3.1). Berger reported his findings on epileptic spikes in 1933 [Berger 33]. The first two groups to apply intensively EEG in the study of patients with epilepsy were those of Herbert Jasper in Providence and Montreal, and Gibbs, Gibbs and Lennox in Chicago. These groups

established the interictal spike as the most specific indicator of epilepsy as early as 1936 [Gibbs 36, Jasper 36].

Herbert Jasper, who was at the time director of the neurophysiology laboratory at Brown University (Providence, Rhode Island), met with Penfield in 1936, shortly after the latter had founded the Montreal Neurological Institute (MNI, 1934). At first, Penfield was sceptical on the ability of EEG to localize epileptogenic lesions. He challenged Jasper to bring some of his patients to Montreal along with his EEG machine. In 1937, Penfield had a laboratory built especially for Jasper at the MNI, and this was the beginning of a very fruitful collaboration that lasted two decades. In particular, Jasper would perform electrocorticograms (ECoG), i.e. recording of the electrical activity directly on the cortex.

The team of Gibbs, Gibbs and Lennox came up with the notion of operating on an electrical focus, i.e. a piece of cortex presenting abnormal EEG activity but no visible lesion. This was against the commonly accepted practice established by Penfield and Foester of only removing tissue with structural pathology. It was therefore difficult to convince surgeons to operate based on electrical activity only; they finally convinced Percival Bailey. The candidates for surgery had anterior temporal focus and were selected mainly on the basis of EEG activity; ECoG was performed intraoperatively to delineate the spiking cortex. In 1951, Bailey and Gibs reported a series with a success rate of just over 50 % [Bailey 51].

Several groups participated in developing a technique that consists in recording the EEG directly in the brain with implanted electrodes: this is the Stereotaxic[1] EEG (SEEG). This technique allows prolonged recordings from deep structures, such as the hippocampus or the amygdala. The leading group was that of Jean Talairach and Jean Bancaud at Hospital Sainte Anne in Paris during the 1960's [Bancaud 65].

A major breakthrough occurred with the clinical use of Magnetic Resonance Imaging (MRI) (see section 4.1). This permitted to visualize lesions such as tumours and hippocampal sclerosis, with high sensitivity and spatial resolution (cf Fig 2.1).

[1]From Greek *stereo*, solid, and *taxis*, arrangement. Stereotaxy permits to define the position of each point inside the head volume with respect to a fixed referential.

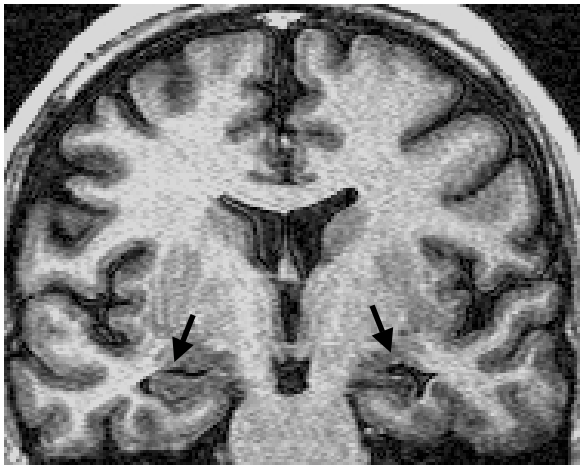

Fig. 2.1 Example of hippocampal atrophy (right arrow), to be compared with the normal side (left arrow). Image courtesy of Dr Eliane Kobayashi.

2.2 The Epileptic Spike

Epilepsy originates from abnormal excitability and abnormal synchronization of populations of neurons. The most dramatic manifestation of epilepsy is the seizure: this is the *ictal*[2] state. The *interictal* epileptic spike is a neuronal discharge that takes place between seizures, and is widely used as a marker of epilepsy. It is a very specific, as it is rarely encountered in non-epileptic subjects.

2.2.1 Basic neuronal mechanisms

The brain is composed of *neurons*, the nerve cells that transmit and process information, and of *neuroglial cells*, which support the activity of the neurons. Each neuron possesses a cell body, many dendrites and one or more axons (cf. Fig. 2.2). The dendrites and the body receive the input from other neurons, and the axon transmits the information to other neurons using a nerve impulse, the action potential.

At rest, there is a difference of electrical potential of approximately 60 mV to 70 mV between the interior and the exterior of the cell body, the interior being more negative (polarization). This difference is established by active mechanisms such as the Na^+/K^+-ATPase pump. The pump moves three sodium ions (Na^+) from the inside to the outside of the cell in exchange for two potassium ions K^+, and uses ATP (adenosine triphosphate)

[2]From Latin *ictus*, stroke.

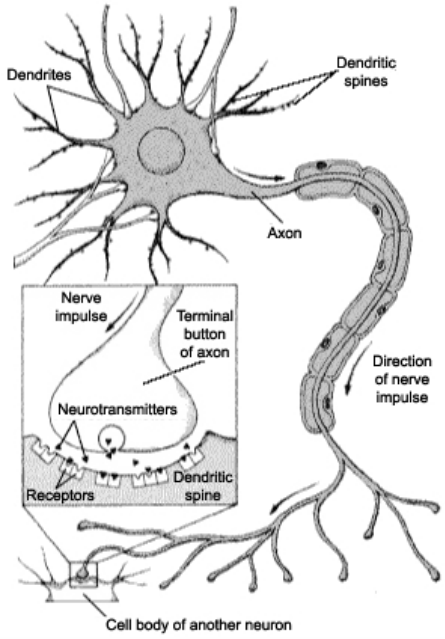

Fig. 2.2 A typical neuron (from www.thebrain.mcgill.ca).

as a source of energy.

Most communication between neurons occurs at the level of chemical interfaces, the *synapses*, located between the axon of a neuron and other neurons. When an action potential reaches a synapse, molecules (*neurotransmitters*) are released through the synaptic junction. These neurotransmitters can be excitatory (e.g. glutamate) or inhibitory (e.g. gamma-aminobutyric acid, GABA). An excitatory molecule raises the intra-neuronal potential (depolarization) by favoring the influx of positive ions through membrane channels[3]. This is the excitatory post-synaptic potential (EPSP). An inhibitory neurotransmitter has the reverse effect (hyperpolarization), producing an inhibitory post-synaptic potential (IPSP). When the region of the first segment of the axon reaches a threshold, the neuron fires one or several action potentials.

There are other types of interaction between neurons, which are non-synaptic and are thought to play a role in epilepsy. The first type is linked to the concentration of ions in the extra-cellular space, which can modify neuronal excitability. For example, an abnormally

[3]The ionic channels are structures permitting the movement of specific ions, that diffuse along a concentration gradient.

elevated level of potassium will affect the efficiency of inhibitory potentials by reducing the gradient across the membrane. This can arise when the efflux of potassium from the cell arising from an action potential is too large to be absorbed by the mechanism of uptake that exists in glial cells. A second type takes place when the membranes of two neurons are so close that the firing of one neuron changes the micro-environment of the other and increases its level of excitability; this is the *ephaptic* effect. A third type of communication happens at the *gap junctions*, or electric junctions, direct connections that let ions pass from one cell to the other.

Most of the energy requirement of neurons is thought to originate from the maintenance of the ionic gradients across the membrane and from the return to resting state after depolarization. There is an increase in blood flow following energy requirement, possibly mediated by nitric oxide (NO) [Gjedde 01].

The neurons of the neocortex are mainly structured in layers (Fig. 2.3). This is a fundamental principle of organization that plays a role in the communication between groups of neurons, in the generation and propagation of epileptic discharges, but also in the generation of EEG (cf. 3.2).

2.2.2 The paroxysmal depolarization shift

(This section is based on reviews [Clark 96] and [Curtis 01]).

Most of our current knowledge on the cellular mechanisms of epilepsy arises from animal models, using electrical stimulation or pro-convulsive substances, and from studies on isolated slices of tissues resected during surgery. In these models, a stereotyped pattern of activity has been observed that is thought to be the cellular correlate of the interictal EEG spike, the "Paroxysmal Depolarization Shift" (PDS).

The PDS corresponds to a very large depolarization - similar to an EPSP but of much larger amplitude and duration - topped by action potentials at a high frequency (cf. Fig. 2.4). The PDS can be followed by an hyperpolarization.

Several types of neurons can produce spontaneous bursts of action potentials, even without any synaptic input. This is observed in some CA3 neurons in the hippocampus even in a situation of normal excitability, and of some deep pyramidal neurons of the neocortex (layers IV and V), this time only when excitability is enhanced. This type of behaviour could be involved in the initiation of the PDS.

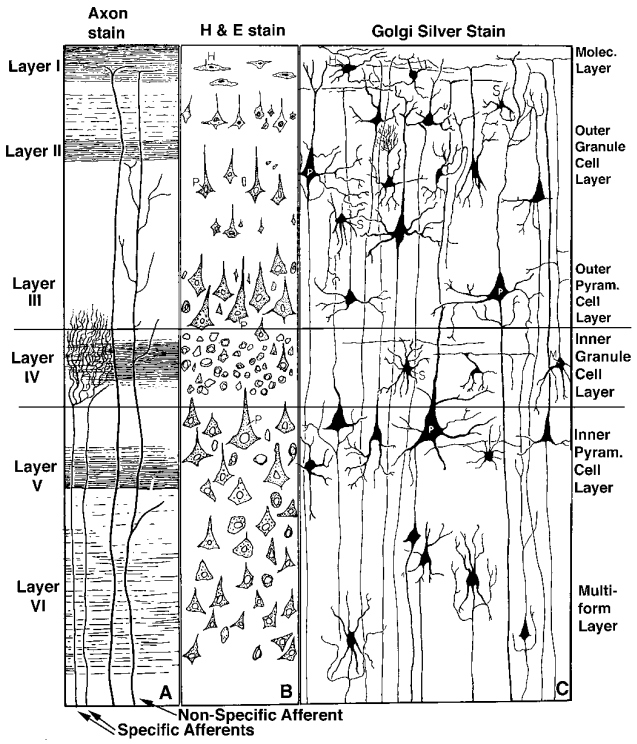

Fig. 2.3 The six layers of the cerebral cortex (from vanat.cvm.umn.edu, University of Minnesota).

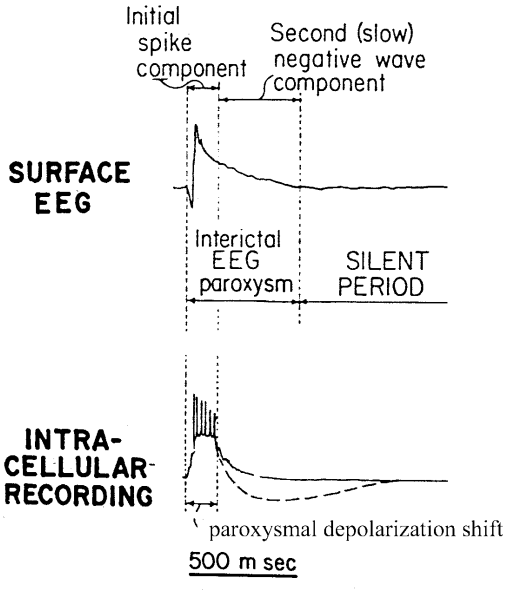

Fig. 2.4 The paroxysmal depolarization shift (modified from [Ayala 70]).

The large depolarizing potential is obtained by the synchronization of a population of neurons, whose mutual influence helps to build up the PDS. This synchronization can take place through recurrent excitatory synaptic interaction; such links are very strong in the hippocampus. Also, it has been observed that an assault to the tissues (for example hippocampal sclerosis or tumour) induces a reconnection of the neurons that could lead to aberrant excitatory (and inhibitory) synapses. Inhibition can also be a potent mechanism for synchronization, which is induced as a rebound response to the hyperpolarization of a population of neurons (in fact, inhibition is thought to be involved in most oscillatory activity). Another mechanism resides in the movement of ions and water across the membrane during the PDS, which produces a swelling of the neurons and glial cells. This reduces the extracellular space and favours non-synaptic influences such as ephaptic effects and elevated potassium concentration (cf. 2.2.1). This is particularly influential in areas where neurons are densely packed, as in the hippocampus.

When enough neurons experience a PDS close to the surface, this is visible on the scalp as an epileptic spike. The propagation of the spike to distant regions can take place though cortico-cortical connections, such as the axonal branches of layer V intrinsically bursting neurons.

The PDS is terminated by a strong polarizing potential, which can be mediated by recurrent inhibitory pathways (fast GABA-mediated inhibition using $GABA_a$ receptors). There is also a more prolonged effect that lasts 1-2 s, which could be mediated by $GABA_b$ receptors. Another possible mechanism is the reduction of gap junction currents induced by changes in pH, which results in a decreased propensity to synchronization. This "silent" period of post-spike inhibition could be what forces a periodicity in trains (*bursts*) of spikes (cf. 2.2.3).

2.2.3 The EEG signal

The scalp EEG spike is usually composed of a fast (spike-like) negative wave, that lasts around 50-80 ms, and a slow positive wave, lasting more than 200 ms (cf. chapters 6, 7 and 8 for examples of spikes). The spikes can occur as single events, or in bursts. In focal epilepsy, it is normally involving only a limited number of electrodes, reflecting the fact that only a limited area of the brain is abnormally active. Nevertheless, a minimum area of cortex needs to be involved in order for the spike to be visible on the surface. The figure

of one square inch (approx. 2.5 x 2.5 cm) has been proposed by Cooper et al. [Cooper 65], who have used a wet skull. They placed electrical sources on the concave side of the skull, and controlled the surface by pinching holes in a plastic sheet placed between the source and the skull. Ebersole confirmed that this figure of around 6 cm^2, although determined in a simplistic way, seems a good estimate of the minimum area required in order to see the spike on the scalp [Ebersole 97].

In some patients, several regions can be involved independently ("multifocal" spikes), or in a fixed pattern of propagation within the cortex. Some stereotyped patterns have been reported in temporal lobe epilepsy in the context of dipole modelling, where the dipole activity seems to propagate from the base of the temporal lobe to the lateral cortex [Baumgartner 95]).

The depth activity recorded with intracerebral electrodes (SEEG) is typically much more diverse that what is seen on the scalp. Indeed, scalp EEG is only a pale reflection of the actual neuronal activity. Some activity may be deep or involve only a limited region of the cortex, and as a consequence may not be visible from the scalp. Also, the activity can start in deep structures such as the hippocampus and become visible on the scalp only after propagation to the neocortex [Alarcon 94].

2.3 Current Methods of Presurgical Evaluation

2.3.1 Patterns of partial epilepsy

The most typical frequent partial epilepsy syndrome is that of mesial temporal lobe epilepsy (MTLE), which involves deep structures (in particular hippocampus and amygdala). MTLE is frequently drug-resistant and can be surgically treated. Around 70-80 % ot the patients become seizure-free, and surgery is probably underused [Lachhwani 03]. MTLE is frequently a bilateral disease, which is an obstacle for surgical intervention. It is therefore necessary to assess if seizures arise on one side and then propagate to the other, or if both sides can generate seizures independently. Lateralization of seizure foci is a very important step because removal of hippocampi bilaterally would lead to irreversible damage, as was demonstrated by the patient H.M.[4].

[4]H.M. was a patient whose two hippocampi were removed following permanent convulsions (status epilepticus). After the operation, he lost his ability to forge new factual memories. He was studied by Brenda Milner, who showed that H.M. could still learn new motor skills: this was a pioneering study for

Another frequent etiology in partial epilepsy is cortical dysplasia[5], a malformation of the cortex that results from an abnormal migration of the nervous cells during maturation of the brain. This type of malformation is very epileptogenic. For this type of epilepsy, seizures are known to arise from within the displastic cortex which needs to be localized and removed, when it is not in an eloquent area. A difficulty is that there can be several such lesions.

Many types of lesions can produce rearrangements of the neurons in their vicinity, where the seizures typically arise. Such lesions can arise from tumours (e.g. astrocytomas, oligodendrogliomas), cerebral vascular diseases or traumatic cerebral injury.

2.3.2 Concepts and principles

Hans Lüders and colleagues have formulated a framework for classifying the zones involved in presurgical evaluation [Rosenow 01] (see Fig. 2.5). This classification is based on early work by J. H. Jackson, and the schools of Montreal, Chicago an London. Important pioneering work has also been performed by Bancaud and Talairach in Paris [Talairach 66].

The *epileptogenic zone* is the portion of cortex that is necessary and sufficient for initiating seizures. This is the zone that needs to be removed or disconnected, with care of preserving "eloquent" cortex, i.e. regions whose removal would lead to post-operative deficits. The epileptogenic zone is quite a theoretical concept, as no current technique enables to define precisely its boundaries - this needs to be inferred from other zones such as those discussed below. Practically, if the patient is seizure-free after the surgical intervention, then the epileptogenic zone is assumed to have been included in the resection. In MTLE, standardized resections can be performed, such as selective amygdalohippocampectomy, where only the amygdala, part of the hippocampus and often parts of neocortex are removed, or the "en-bloc" resection, where a large part of the temporal lobe is removed.

The *symptomatogenic zone* is the region that produces the clinical symptoms when activated by ictal discharges. Until the appearance of modern diagnostic tools, this was the main source of information for localizing the epileptogenic zone. There is still important localizing information that can be gained from the symptoms preceding or at the start of the seizures. For example, a sensation of tingling in the hand indicates an involvement of the contralateral hand area. However, the symptomatogenic and the epileptogenic zones

establishing both the role of the hippocampus and the existence of different types of memory systems.

[5]From Greek *dys*, bad, and *plasia*, conformation.

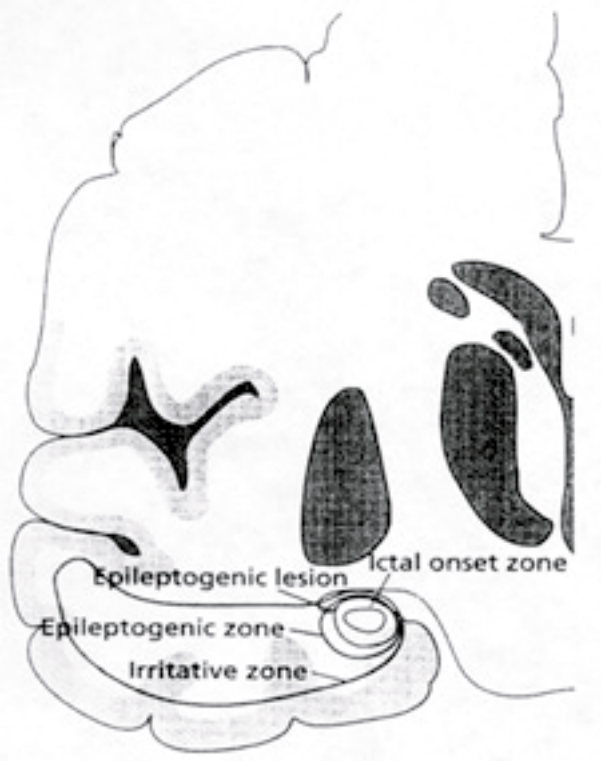

Fig. 2.5 The different zones in presurgical evaluation (from [Dinner 98])

can be distinct, as seizures may start in a region with no clinical symptom ("silent cortex") and then propagate to other regions where symptoms are produced.

The *lesional zone* is the region of the brain where structural damage can be seen. The most common lesion is the hippocampal sclerosis (cf. Fig. 2.1), and unilateral hippocampal sclerosis with concordant symptoms is a very good indication for surgery.

The *irritative zone* is the region where interictal epileptic spikes are produced. This region is often large and does not need to be fully resected for seizure relief. For example, in temporal lobe epilepsy, spikes are often observed both in the hippocampus (this requires depth recordings) and in the lateral part of the temporal lobe (this activity is visible on scalp EEG). Often, the resection of the region of the hippocampus is sufficient to render the patient seizure-free.

The *seizure onset zone* is the region from where the seizures actually start. It has been observed that the resection of this zone is usually not sufficient for abolishing the seizures. Indeed, other zones can have a potential for seizure generation, which only becomes apparent after the resection of the seizure onset zone.

The *functional deficit zone* is the region that presents impaired functioning during the interictal period. The relation with the epileptogenic zone is complex, but concordance with the other described zones can be a good indicator of lateralization and localization.

Another interesting approach was developed by Jean Talairach, Jean Bancaud and their students Patrick Chauvel and Claudio Munari. In their view, the epileptogenic zone should be seen as a network of interconnected areas, including relays and pacemaker areas. The epileptic state arises as a property of this network, and several regions may be involved in the generation of seizures [Isnard 00]. This approach has led for example to the concept of fronto-temporal epilepsy [Bancaud 92].

2.3.3 Evaluation tools

An important step in the evaluation of an epileptic patient remains a thorough neurological evaluation, that aims at gathering information such as seizure description and frequency, familial antecedent, accidents, frequency and history of seizures, etc. Then, the main tools for investigating patients with refractory epilepsy are prolonged video-EEG recording and Magnetic Resonance Imaging (MRI).

In the long-term monitoring unit, the EEG can be recorded for several days, usually with

a lowered medication in order to facilitate the recording of seizures. The video enables the study of the clinical symptoms, and the clinical personnel can interact with the patient at the early stage of the seizure to assess functional impairments. The EEG can be processed online in order to detect automatically the spikes and seizures, which helps in reviewing the large amount of data [Gotman 99].

MRI allows the visualization with excellent resolution of lesions such as tumours, cortical displasia and hippocampal atrophy. Quantitative methods can be used to increase the capacity of MRI to distinguish between normal and abnormal tissue. For example, the measurement of the volume of mesial structures can help finding atrophy [Cendes 97]; automated texture analysis can point to cortical malformations [Antel 03].

Recently, functional MRI has been proposed as a way to map the eloquent cortex, i.e. parts of the brain whose removal would lead to functional deficit [Bittar 99].

Many other imaging techniques were proposed over the years for the non-invasive investigation of epileptic patients. Computerized X-Ray tomography (CT) was developed in the 1970's and permitted to visualize tumours and haemorrhages. Positron Emission Tomography (PET) enables to study the decrease in metabolism usually associated with interictal activity [Engel 91]. This method is of great potential as it also permits to target the sites of specific neurotransmitters which can be altered in association with epilepsy. With Single Photon Emission Tomography (SPECT), the patients can be injected at the time of seizure onset. The radioactive tracers is fixed in the regions of higher perfusion due to increased metabolic activity, and can be imaged several hours later [Harvey 93].

2.4 Clinical Significance of the Interictal Spike

The main targets of presurgical evaluation are usually the lesional zone and the ictal onset zone. However, as pointed out in 2.3.2, the resection of these zones alone may not lead to seizure freedom. Therefore, it is potentially informative to delineate all the tissues prone to epileptic activity. It is possible that the irritative zone gives an indication of regions with a low threshold for seizure generation that could be regions of potential seizure onset.

Interictal activity can be visualized during the operation with the ECoG. This can be used for delineating the amount of cortex to be removed, i.e. "tailoring" the resection intra-operatively [Penfield 54, Kanner 95, McKhann 00] (this is to be contrasted with the standardized resections). In fact, for many years surgery was performed quite successfully

on the basis of spiking alone, as at this time seizures were almost never recorded. For example, Theodore Rasmussen at the MNI performed hundreds of such operations.

The link between ictal and interictal activity is not completely clear. One view is that the interictal spike is a mini-seizure. Indeed, the spikes involve networks that may be related to the epileptic pathways [Badier 95]; Alarcon et al. have shown that the propagation of interictal spikes could be similar to that of seizures [Alarcon 94]. From a different viewpoint, it has been proposed recently that the interictal spiking helps in fact controlling the occurrence of seizures by maintaining inhibition within the epileptic tissue [Curtis 01, Avoli 01]. Gotman and Marciani have shown that the frequency of spikes is higher after a seizure [Gotman 85], and Jansky et al. have shown that the lateralization of the preceding seizure influenced that of the spikes [Janszky 01]. Rosati et al. pointed out a correlation between the severity of the epileptic state and the number of spikes (the patients with very few spikes had a less severe epilepsy) [Rosati 03]. In any case, the extent of interictal activity seems to give an indication on the amount of tissue prone to epileptic activity.

A more pragmatic use of the interictal spikes is in the lateralization of the epileptogenic zone (cf. 2.3.1). Indeed, it has been shown that concordant lateralization of interictal activity and MRI abnormalities correlates with success of surgery when the patient is operated on this side [Gilliam 97]. Also, remnant interictal epileptic activity in the temporal neocortex (lateral part of the temporal lobe) is correlated with the patient still having seizures [Kinay 04]. This suggests again that the interictal spike is a marker of epileptogenicity.

2.5 Conclusion

The epileptic spike is a very common manifestation of epilepsy; it also usually happens with a much higher frequency than the seizures. The links with the phenomena of seizure initiation and with the evolution of the epileptic syndrome are not completely clear, but there are indications of relationships between the interictal spiking and the ictal state. As a consequence, the study of interictal activity is an important aspect of presurgical evaluation of epileptic patients.

The main tool for investigating the interictal discharges remains the EEG. The traditional visual interpretation of the location of interictal spikes remains prevalent. However, signal processing techniques have been proposed to increase the precision of the localization of the cortical regions producing the interictal spikes for a given patient (cf. chapter 3).

Functional imaging techniques, such as PET, SPECT and more recently fMRI are also of increasing interest (cf. chapter 4).

Chapter 3

EEG Source Localization

As mentioned in the previous chapter, the electroencephalogram remains a technique of choice in the presurgical evaluation of epilepsy, as it permits to visualize non-invasively the epileptic discharges. The main method for interpreting the EEG data is the visual inspection of the traces. The distribution of the potentials on the scalp can be related to the actual generators, keeping in mind that the maximum of potential does not automatically imply an underlying source. Indeed, careful consideration of the possible conformation of the generators and of the propagation of electrical currents is required [Gloor 85]. We will present in this chapter the EEG technique, as well as methods that have been proposed to refine the EEG-based localization by obtaining results directly within the brain.

3.1 A Brief History of Electroencephalography

(Main source: [Niedermeyer 99])

Emil Dubois-Reymond (1818-1896) is the German founder of experimental neurophysiology. He studied muscle contraction, nerve conduction, and coined the expression "negative variation" for the unexpected decrease in current intensity observed during muscle contraction (1843). He collaborated with Hermann von Helmholtz, a medically trained multi-disciplinary scientist who accurately measured the conductivity of nerve fibres. The first electrophysiologists were using simple galvanometers that could measure continuous (DC) currents with a coil moving inside a fixed magnet.

Richard Caton (1842-1926), in Liverpool, was the first to measure the electrical activity

of the brain, principally on rabbits. He observed differences of potential between two points on the scalp or between the surface of the brain and deep structures. He also observed that "when any part of the grey matter is in a state of functional activity, its electric current usually exhibits negative variation" [Caton 75], and opened the way to electrophysiological mapping.

Hans Berger (1873-1941) performed the first recordings of the electrical activity of the human brain. He started by studying subjects with large skull defects, but soon realized that brain potentials could also be recorded through a defect-free skull. He used double coil galvanometers with non-polarizable electrodes and produced paper tracings recorded for one channel ([Berger 33], translated in [Berger 69]). Berger coined the word *elektrenkephalogram*, and produced observations on the alpha wave, sleep spindles, fluctuation of consciousness and various brain disorders, including some epileptic activity. In Berlin, M.H. Fisher and A.E. Kornmüller produced the first EEG study on epileptic spikes, following poisoning with convulsive substances on the cortex of animals (1933, 1935). They used the ink-writing differential amplifier designed by J.F. Toennies (1902-1970). Kornmüller pointed out differences between regions of the brain and emphasized the importance of multi-channel recordings.

In the 1930's and 1940's, in Harvard, William G. Lennox, Frederick Gibbs and Erna L. Gibbs made a breakthrough in clinical EEG by studying intensively epileptic patients and their paroxysmal discharges. They used a three-channel amplifier writing on rolls of paper built by Albert Grass. Another pioneer of the use of EEG in epilepsy was Herbert Jasper, who set up an EEG laboratory at the Montreal Neurological Institute in 1939 [Jasper 41]. In 1948, F. Gibbs studied the anterior temporal interictal spikes [Gibbs 48]. Around the same time, Henri Gastaut in Marseille determined the response threshold in photosensitive epilepsy.

The 1950's saw an explosion in the use of clinical EEG. The main groups in North America were those of F. Gibbs and E.L. Gibbs in Chicago and of Herbert Jasper and Wilder Penfield in Montreal. Gibbs and Gibbs took part in the development of depth EEG, while Jasper and Penfield perfected intraoperative electrocorticography and became leaders in focal epilepsy surgery. In Europe, the great centers were Queen Square in London, with William Cobb, and the Salpêtrière Hospital in Paris with Jean Talairach, Jean Bancaud and Antoine Rémond. Later, Rémond took part in the computerization of EEG, a tendency that became prominent from the 1970's on [Gotman 97].

3.2 Origin of EEG Potentials

3.2.1 Neuronal currents

As we presented in 2.2.1, an action potential arriving at the synapse results in a post-synaptic increase (depolarization) or decrease (hyperpolarization) of the resting potential, depending on the type of synapse (resp. excitatory or inhibitory). These are the Excitatory/Inhibitory Post-Synaptic Potentials (EPSP/IPSP), and are caused by an active movement of ions across the neuronal membrane. This change in the ionic density at the level of the membrane creates ionic currents both inside and outside the neuron.

When a large number of neurons experience post-synaptic potentials, significant currents start to flow in the surrounding tissue. If moreover these neurons are close enough to the surface of the head, the currents produce potentials at a level that can be recorded with scalp EEG. This is the case with the pyramidal neurons of layer IV that are aligned in parallel and are very inter-connected. These pyramidal neurons are in fact thought to be the main cells responsible for scalp EEG potentials [Speckmann 04].

The arrangement in a layer of parallel neurons active together implies that there is *spatial summation*. It is equally important to have *temporal summation*, i.e. that the neuronal potentials occur simultaneously. This is the reason why the action potentials, which are very brief and therefore more unlikely to occur at the exact same time across neurons, are not considered to contribute significantly to the EEG. In other words, the EEG can be thought of as a low-pass filtered version of the neuronal activity, which explains the $1/f$ structure of the EEG spectrum.

During an EPSP, the membrane at the level of the synapse acts as an active current sink with respect to the extracellular medium, i.e. a place where currents flow out of the medium (positive ions exit the medium to enter the neuron). The rest of the neuronal membrane acts as a passive source, where on the contrary current flow out of the neuron. Pyramidal cells are often asymmetrical with a long vertical apical dendrite: this configuration is very similar to a current dipole perpendicular to the surface of the cortex. The location and type of synaptic input determine the sign of the potentials measured on the surface (cf Fig. 3.1).

A set of active pyramidal cells can be modelled electrically as a dipole layer [Gloor 85].

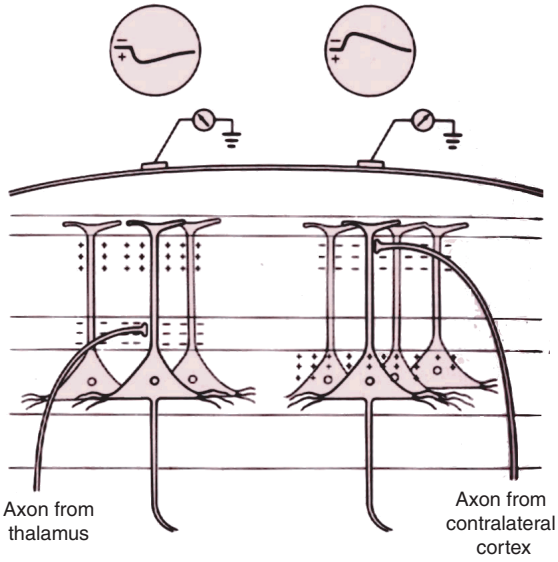

Fig. 3.1 The potentials generated by pyramidal neurons receiving EPSP either at the apical dendrite (left) or the soma (right) (from www.acm.org).

3.2.2 Physics of EEG

We have seen that the active neurons act as current sources. This can be represented by a source current density $\vec{j}_S$. These sources produce currents inside the volume of the head that can be described by an electric field $\vec{E}$ [Nunez 81].

According to the local version of Ohm's law for a linear medium with conductivity σ (S/m), the volume current is $\vec{j}_V = \sigma\vec{E}$. The total current $\vec{j}$ is the sum of the impressed (source) current and the volume current:

$$\vec{j} = \vec{j}_S + \sigma\vec{E}. \tag{3.1}$$

The Maxwell equations for an electric field state that

$$\nabla \cdot \vec{E} = \sigma/\epsilon \tag{3.2}$$

and

$$\nabla \times \vec{E} = -\frac{\partial \vec{B}}{\partial t}, \tag{3.3}$$

where ∇ is the gradient operator (spatial partial derivatives: $\nabla = \partial/\partial x\ \vec{x} + \partial/\partial y\ \vec{y} +$

$\partial/\partial z\ \vec{z}$), ϵ the permittivity and $\vec{B}$ the magnetic field [Zhukov 99]. For the low frequency range that is typically of interest in EEG (less than 100 Hz), one can use the quasi-static approximation for (3.3):

$$\nabla \times \vec{E} = 0. \tag{3.4}$$

This means that the field can be described as the derivative of a potential function V:

$$\vec{E} = -\nabla V. \tag{3.5}$$

Finally, the law of conservation of charges states that

$$\nabla \cdot \vec{j} + \frac{\partial \rho}{\partial t} = 0, \tag{3.6}$$

where ρ is the density of charges. If we suppose that there is no accumulation of charges at a given point in the volume, then

$$\nabla \cdot \vec{j} = 0, \tag{3.7}$$

which means that the sum of the current that enters a given elementary volume and of the current that exits the volume is zero (the local equivalent of Kirchoff's laws for circuits).

If we combine equations (3.7), (3.1) and (3.5), we obtain the Poisson equation for the electric potential:

$$\nabla \cdot (\sigma \nabla V) = \nabla \cdot (\vec{j_S}). \tag{3.8}$$

Equations (3.7) and (3.4) imply conditions at the boundaries between media of different conductivity (e.g. between brain and skull or between skull and skin):

$$\vec{J}_{1n} = \vec{J}_{2n} \tag{3.9}$$

and

$$\vec{E}_{1t} = \vec{E}_{2t}, \tag{3.10}$$

where n refers to the normal component and t to the component tangential to the surface.

3.3 Current Techniques of Source Localization

All EEG source localization methods make use of models of the sources and of the volume conductor in which the currents propagate. This serves to solve the *forward problem*, where the potentials on the scalp created by a given source are computed. The conducting medium is assumed to be purely resistive (i.e. capacitive effects are neglected), and electric fields are considered to propagate instantaneously (i.e. the variation of one source affects the potentials measured at each electrode with no delay) [Nunez 81].

The forward problem serves in turn to solve the *inverse problem*, i.e. to find the location of the sources inside the brain given the potentials at the surface of the head. This type of problem falls inside the category of "ill-posed" Problems. According to the definition of Hadamard, a problem is well-posed if

1. It has a solution
2. The solution is unique
3. The solution depends continuously on the data

Criterion 2 is not fulfilled, because an infinity of configurations of electrical sources inside a volume conductor can produce the exact same potential distribution at the surface of the conductor. Moreover, criterion 3 is also not met, which means that small errors in the measurements can cause large errors in the results of the inverse problem.

Fortunately, the use of a source model and regularization techniques (such as those proposed by Tikhonov [Tikhonov 77]) reduce greatly the ambiguity. Practically, given some head and source models, the configuration that explains "best" the data under specific assumptions is obtained.

Source localization in EEG and Magnetoencephalography (MEG) make use of the same techniques and mathematical formalism. Therefore, this field is often referred to as the *electromagnetic inverse problem* [Baillet 01a].

3.3.1 Source and head models

Source model

As was mentioned in 3.2, a piece of active cortex behaves as a dipole layer. This layer, seen from a remote location, produces potentials very similar to those of a single dipole [Brazier 49], even for relatively extended sources [de Munck 98] (cf. Fig. 3.2). If one as-

sumes that only a few restricted areas are active simultaneously, then the EEG potentials can be modelled as a small set of equivalent dipoles [Henderson 75]. Under the (very theoretical) assumption of a few activated *true* dipoles, the sources can be identified uniquely [El Badia 00].

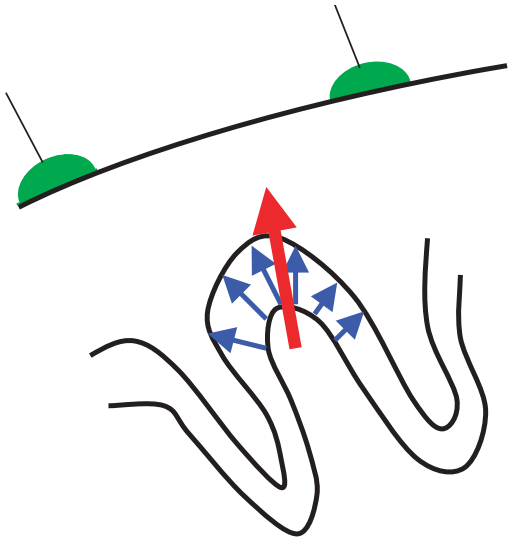

Fig. 3.2 Schematic view of the cortex, along with the scalp and electrodes (in green). The activated neurons can be represented by current dipoles (blue). A patch of cortex can be modelled by an equivalent dipole (red).

The assumption of dipolar sources can be at the expense of some localization error though, as a dipole equivalent to a large area of cortex can be at a distance from the actual source layer. Also, in the case of multiple sources, estimating the number of dipoles is often a difficult task. Finally, the assumption of focal sources can be inappropriate, for example in complex cognitive processes or in widespread epileptic discharges.

These considerations have led some workers to prefer "distributed" sources where a large number of dipoles (several thousand) are placed evenly in the head, either in the whole brain volume or along the surface of the cortex. The information on the location and orientation of the cortex can be obtained from magnetic resonance images [Dale 93]. As the number of unknown variables is then much larger than the number of measurement points (the electrodes), some additional constraints on the smoothness or amplitude of the current distribution are needed (cf. 3.3.2).

The constraints used in distributed sources modelling were introduced mainly for com-

putational purposes, and their link to actual physiological parameters is not very strong. An interesting alternative is to use pieces of cortex, or *patches*, containing a set of contiguous dipoles perpendicular to the cortex.

Head model

The head model consists of a representation of the geometry of the head and of the electrical conductivity of the elements of the head volume, in order to solve the Poisson equation (3.8). The classical model is composed of a set of concentric spheres representing the scalp, skull and brain, and delimiting volumes with the corresponding conductivity, assumed to be homogeneous inside each compartment. One advantage of this model is that it permits analytical computation of the potential produced at the surface of the sphere by a dipole at any location inside the inner sphere [Kavanagh 78].

More recently, realistic head models have been designed that take into account the actual shape of the head, skull and brain compartments. Discrete meshes are obtained based on magnetic resonance images. When only the surfaces of the compartments are modelled with two-dimensional elements (e.g., triangles), the technique is referred to as the Boundary Element Method (BEM, [Barnard 67]). When the whole volume is meshed with three-dimensional elements, this is the Finite Element Method (FEM, [Yan 91]). The FEM is more demanding computationally than the BEM but permits models with a more complex geometry, and can take into account tissue anisotropy such as that of the skull [Marin 98].

The formula used for computing the potential at a given point $\vec{r}$ of a surface $S_i, i \in 1...m$ (S_1 is the scalp surface; S_2, S_3 ... are surfaces included within each other that model for example the skull, brain, ventricles) is [Geselowitz 67, Hämäläinen 89]:

$$(\sigma_i^- + \sigma_i^+)\Phi(\vec{r}) = 2\sigma_m\Phi_0(\vec{r}) + \frac{1}{2\pi}\sum_{j=1}^{m}(\sigma_j^- - \sigma_j^+)\int_{S_j} V(\vec{r}\,')\frac{\vec{r}\,' - \vec{r}}{|\vec{r}\,' - \vec{r}|^3}\cdot\vec{n}dS \qquad (3.11)$$

where σ_i^- and σ_i^+ are the conductivities inside and outside the surface S_i respectively, Φ_0 is the potential generated by the source in an infinite uniform medium, and $\vec{n}$ is a vector normal to the surface at a given point. In the case of the simple current dipole $\vec{p}$, this

potential is

$$\Phi_0(\vec{r}) = \frac{1}{4\pi\sigma_0} \frac{\vec{p} \cdot (\vec{r} - \vec{r}_0)}{|\vec{r} - \vec{r}_0|^3} \tag{3.12}$$

with σ_0 unit conductivity.

In order to solve the BEM numerically, the surfaces S_i are divided in small triangles and the integral is approximated by a discrete sum.

3.3.2 Solving the inverse problem

Dipolar method

In this method, sources are assumed to be made of a few distinct electrical dipoles. One dipole at a given time point is defined by its location, orientation and strength (6 parameters). As the medium is assumed to be purely resistive, the observed potentials are the sum of the contributions of each dipole:

$$\mathbf{Y} = \mathbf{X}(\Theta)\mathbf{B} + \mathbf{E}, \tag{3.13}$$

where $\mathbf{Y}$ is the spatiotemporal data matrix (n channels $\times$ p time points) that usually results from the average of k identical events in order to improve the signal-to-noise ratio, $\mathbf{X}$ is the matrix of spatial components (n channels $\times$ d dipoles) that contains the potentials generated by each dipole, Θ contains the parameters of the dipoles, $\mathbf{B}$ contains the dipole time course (d dipoles $\times$ p time points) and $\mathbf{E}$ is the error matrix (n channels $\times$ p time points) (cf. Fig. 3.3).

The maximum number of sources that can be localized within the linear model of type 3.13 was defined by [Wax 89] for a one-dimensional array (one parameter per source) and by [Hochwald 96] for the general case of multidimensional arrays. We will use here the simple condition that the number of parameters to estimate must be smaller than the number of equations (a condition that can be violated in some circumstances according to [Hochwald 96]), and will consider only the noise-free case.

The number of independent equations in the equation $\mathbf{Y} = \mathbf{XB}$ is $(n-1)\eta$, with η the rank of temporal covariance matrix of the data ($\mathbf{Y}^T\mathbf{Y}$). There are only $(n-1)$ independent channels as recordings are always made with respect to a common reference channel. As the number of independent parameters to estimate is $5d + \eta d$, one cannot estimate more than $(n-1)\eta/(5+\eta)$ sources. If all channels and all time points were independent, for

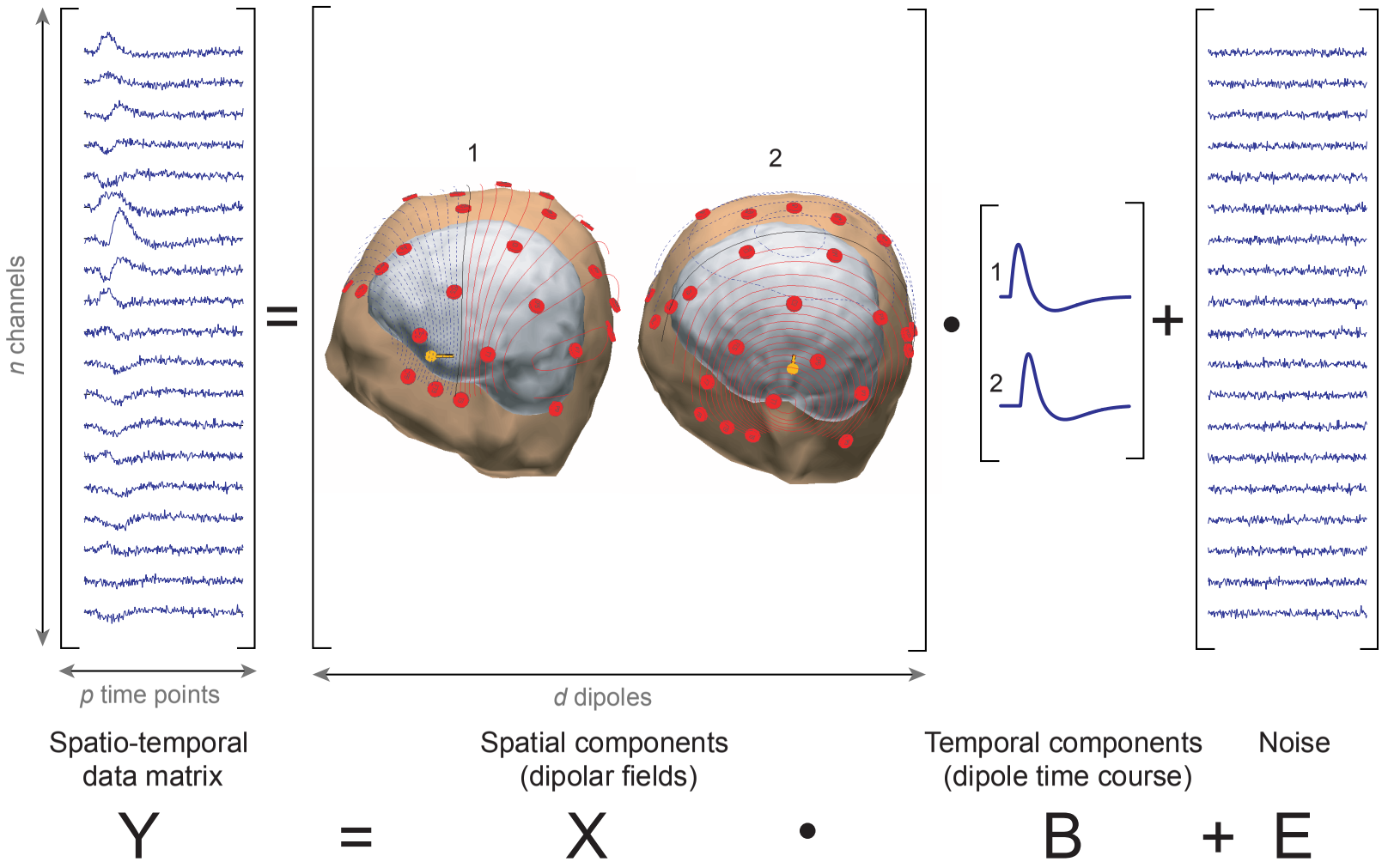

Fig. 3.3 The linear model for dipolar source localization, for a schematic example (simulated sources and white noise). The data matrix is represented by fixed spatial components (the dipole fields) with corresponding time courses. Dipole 1 is an example of a tangential source, located in the anterior temporal lobe. Dipole 2 is an example of a radial source, and is located on the lateral part of the temporal lobe.

$n = 64$ channels and $p = 20$ time points at 200 Hz (100 ms), and for sources that are not correlated ($\eta = p$), one would be able to separate $63 * 20/(5 + 20) = 50$ sources. However, data are very correlated in space and time. If one assumes in a very rough approximation that the smoothness is of the order of 5 time points and one inter-electrode distance, which involves around 5 electrodes, then a more realistic figure is $(63/5) * 4/(5 + 4) \simeq 5$ dipoles. Moreover, the potentials created by close dipoles are very similar, which is a handicap for separating close sources in the presence of noise.

One can consider that a dipole represents a patch of cortex that is stably activated during the time window, i.e. that the extent of the patch and the distribution of currents on the patch stays the same. This means that the dipole location and orientation can be held fixed in the time window; this is the basis of "spatio-temporal" dipole modelling [Scherg 85]. This lowers drastically the number of parameters to estimate per dipole ($5 + p$ instead of $6p$ in the uncorrelated case) and renders the method more robust with respect to noise. Another option is the *regional source*: three colocalized and orthogonal dipoles represent all possible dipolar activity in the region of the source [Scherg , Mosher 92].

Classically, the time course of the dipoles, given location and orientation parameters, are estimated by the ordinary least squares method:

$$\hat{\mathbf{B}} = (\mathbf{X}^T\mathbf{X})^{-1}\mathbf{X}^T\mathbf{Y}. \tag{3.14}$$

In geometrical terms, one finds with (3.14) the point in the subspace spanned by the dipole models that is closest to the signal, for each instant. In practice, the matrix $(\mathbf{X}^T\mathbf{X})$ cannot be inverted because of the reference issue mentioned above, and a pseudo-inverse must be used instead.

Once the number of dipoles is specified, the locations (and orientation for spatio-temporal modelling) can be searched using a non-linear minimization (for example the simplex method). For a given set of localization and orientation parameters, the fit is performed linearly using (3.14). The goodness of fit of a particular configuration is measured by the residual variance

$$RV = 100 \cdot \frac{tr[(\mathbf{Y} - \mathbf{X}\hat{\mathbf{B}})^T(\mathbf{Y} - \mathbf{X}\hat{\mathbf{B}})]}{tr(\mathbf{Y}^T\mathbf{Y})}\ \% \tag{3.15}$$

i.e. the percentage of the signal energy that has not been explained by the model.

The advantage of the dipolar method is its simplicity. One drawback is that one needs to specify *a priori* the number of sources. Other drawbacks are the existence of local minima in the optimization process and the requirement for the sources to be of small extent.

Maximum likelihood

The formulation (3.14) gives an optimal (unbiased) estimate only if the noise is white, i.e. of equal amplitude across channels and uncorrelated from channel to channel, and Gaussian. In reality, there are strong correlations both in time and space, which means that one risks to overfit the data by explaining part of the noise.

Lütkenhöner [Lutkenhoner 98b] proposed to take into account the spatial covariance of the noise. This is the *maximum likelihood* approach, which is equivalent to rendering the noise white spatially (prewhitening). He found that the estimates of dipole location for different realizations of the noise were much more stable with prewhitening .

Maximum likelihood is a general technique for estimation of parameters of statistical models. The likelihood is the probability of the observations given the observations, seen as a function of the parameters. In the case of the linear model (3.13), the likelihood $\mathcal{L}$ is the probability of the residuals to be only noise. For one time point and assuming Gaussian noise with spatial covariance Σ, we obtain:

$$\mathcal{L}(\Theta) = \frac{1}{\sqrt{(2\pi)^n |\Sigma|}} e^{-\frac{1}{2}(\mathbf{Y}-\mathbf{X}(\Theta)\mathbf{B})^T \Sigma^{-1} (\mathbf{Y}-\mathbf{X}(\Theta)\mathbf{B})}, \tag{3.16}$$

which is maximized when the quantity

$$(\mathbf{Y} - \mathbf{X}(\Theta)\mathbf{B})^T \Sigma^{-1} (\mathbf{Y} - \mathbf{X}(\Theta)\mathbf{B}) \tag{3.17}$$

is minimum. This is achieved by

$$\hat{\mathbf{B}}_{gls} = (\mathbf{X}^T \Sigma^{-1} \mathbf{X})^{-1} \mathbf{X}^T \Sigma^{-1} \mathbf{Y}, \tag{3.18}$$

which is a generalization of (3.14) for spatially correlated noise. As mentioned previously, this is the same as multiplying the data $\mathbf{Y}$ and the spatial components $\mathbf{X}$ by $\mathbf{U}$ ("prewhitening"), with $\mathbf{U}^T\mathbf{U} = \Sigma^{-1}$, and then applying (3.14). Figure 3.4 presents Gaussian distributions in two dimensions and the effect of prewhitening.

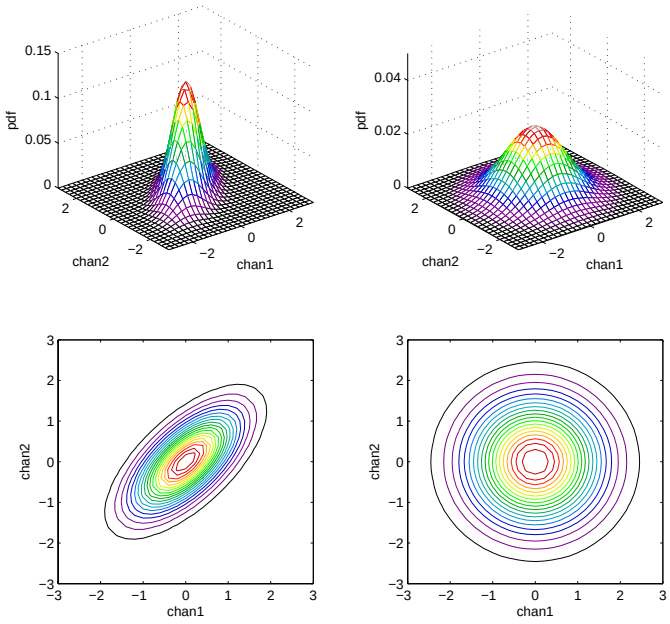

Fig. 3.4 Gaussian distribution in two dimensions (two channels). Upper row: three-dimensional surface, lower row: contour plot. Left: correlated case (40 % of correlation), Right: uncorrelated (white) case. Fitting data with correlated noise will tend to overfit the noise in the direction of maximum variance (in this example, the line $chan2 = chan1$). Prewhitening is the transformation from the correlated case to the uncorrelated case.

MUSIC

The contribution of each source in (3.13) lies within a subspace of the n-dimensional space of all possible single-time measurements (n number of electrodes). For example, in the simple case of one dipole with amplitude varying in time but with fixed location L_0 and orientation M_0, the subspace is one-dimensional: every potential produced by the dipole is proportional to the potential produced by a unit dipole (L_0, M_0).

The Multiple Signal Classification (MUSIC, [Schmidt 86], [Mosher 92]) algorithm assumes that in (3.13) the observed signal $\mathbf{Y}$ originates from s sources having time courses that are uncorrelated both between each other and with the noise. In that case, the first s spatial components of a Principal Component Analysis (PCA) of $\mathbf{Y}$ constitute an orthogonal basis for the subspace spanned by the sources, called the *signal subspace* (cf. Fig. 3.5). One can then scan the head with a probe dipole and compute the inverse of the angle between the dipole subspace and the signal subspace. True sources should give very small angles, and can be identified as peaks in the result of the scan. The advantage of this method is to permit a simple (low-dimensional) one-dipole scan. The major constraint is that the temporal courses of the sources need to be uncorrelated.

Distributed sources

The distributed sources model has the same formulation as (3.13), but this time $\mathbf{X}$ contains the potentials created by a very large number of dipoles distributed on the cortical surface, of the order of a few thousand ($d \gg n$). As was mentioned at the start of the section, this leads to many more unknown parameters than measured data, with an infinite number of possible solutions. This requires further constraints in order to have a system both solvable and stable with respect to noise (review in [Gulrajani 98], p. 577).

Hamalainen and Ilmoniemi proposed to look for the solution that has minimum energy: this is the *minimum norm* assumption [Hämäläinen 94], or L_2 norm (i.e. root of squared elements). This is the simplest form of regularization as proposed by Tikhonov for ill-posed problems [Tikhonov 77]. The cost function to minimize is then, at a given time point:

$$cost = \|\mathbf{Y} - \mathbf{XB}\|^2 + \lambda\|\mathbf{X}\|^2 \tag{3.19}$$

with $\mathbf{Y}$ measured potentials, $\mathbf{X}$ matrix of the fields produced by unit dipoles (*lead field*

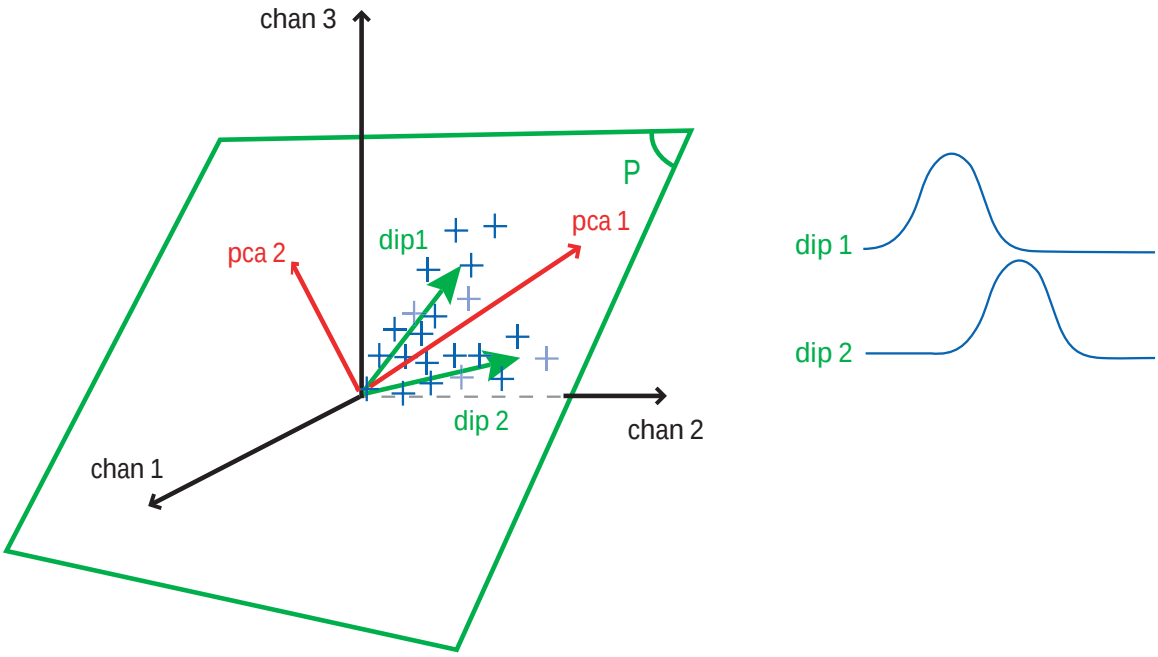

Fig. 3.5 Schematic view of the MUSIC technique. At a given time point, the EEG measurement constitutes one point in the space of the captors (here, there are only three channels: $chan_1$, $chan_2$ and $chan_3$). We assume the sources are two dipoles dip_1 and dip_2 (green vectors) with asynchronous time courses (shown on the right). All possible linear combinations of dip_1 and dip_2 lie within the plane P defined by (dip_1, dip_2). The measured signal is the sum of the two dipolar sources plus noise, and the corresponding points (blue crosses) are close to the plane P. The first PCA vector pca_1 follows the direction of maximum variance, approximately in between dip_1 and dip_2, and close to P. The second PCA vector is orthogonal to pca_1 by construction, and also close to P as it explains the remaining variance. If one scans the head with a single probe dipole $\vec{d}$ and measures the angle between $\vec{d}$ and the (pca_1, pca_2) plane, this angle will be very small for $\vec{d} = dip_1$ and $\vec{d} = dip_2$.

matrix), **B** source amplitudes and λ regularization parameter. The value of λ sets the weight given to the criterion of minimum norm. It is tuned as a balance between the goodness of fit (at the left of the plus sign) and the minimum norm term (at the right). One method to find lambda is the "L curve", where the minimum norm term is plotted as a function of the residuals. This curve is usually L-shaped, and the corner of the L is used as an optimum value of λ.

The minimum norm formulation has a linear solution computable directly. There are also non-linear distributed models, for example the L_1 method, where the sum of the absolute values is used instead of the squared values in 3.19 [Fuchs 99]. the L_1 method gives a more focal solution than the minimum norm (or L_2).

In the LORETA method (Low Resolution Brain Electric Tomography), the constraint is that of maximum spatial smoothness [Pascual-Marqui 94] (minimization of the spatial Laplacian).

The distributed sources methods do not require specification of the number of sources, but need heavy spatial constraints that may not be physiologically motivated and that are sensitive to the choice of the regularization parameter λ.

Bayesian methods

The Bayesian framework enables the computation (within a proportionality factor) of the probability of a certain set of sources given the measured data and the *a priori* knowledge of the system (noise, source location, etc...). It is based on an application of Bayes formula:

$$P(\mathbf{\Theta}|\mathbf{Y}) \sim P(\mathbf{Y}|\mathbf{\Theta})P(\mathbf{\Theta}), \tag{3.20}$$

where $\mathbf{Y}$ is the observed data and Θ the set of parameters (e.g. number and location of sources). One can then compute the maximum *a posteriori* estimator that maximizes 3.20 [Radich 95]. An interesting possibility is to display different sets of sources and their respective probability [Schmidt 99] (see next section).

The solutions for the linear distributed sources methods can be derived within the Bayesian framework [Baillet 01a], which is interesting in the context of data fusion (see section 3.3.3). Indeed, the probability of the dipole amplitudes given the measurement is, similarly to (3.20):

$$P(\mathbf{B}|\mathbf{Y};\alpha,\beta) \sim P(\mathbf{Y}|\mathbf{B};\alpha)P(\mathbf{B}|\beta). \tag{3.21}$$

where α and β are function of the *a priori* covariance of noise and sources, respectively.

Under the assumption of white Gaussian noise (cf (3.16)) and Gaussian dipole amplitude with covariance matrix $\mathbf{C}$, one obtains for the (negative log of the) posterior probability

$$-log(P(\mathbf{B}|\mathbf{Y};\alpha,\beta)) \sim \alpha(\mathbf{Y}-\mathbf{XB})^T(\mathbf{Y}-\mathbf{XB}) + \beta\mathbf{B}^T\mathbf{C}^{-1}\mathbf{B}, \tag{3.22}$$

The quantity (3.22) is minimized (i.e. maximum *a posteriori* probability) with a solution of the form:

$$\hat{\mathbf{B}} = \mathbf{C}^{-1}\mathbf{X}^T(\mathbf{X}\mathbf{C}^{-1}\mathbf{X}^T + \lambda\mathbf{I})^{-1}\mathbf{Y} \tag{3.23}$$

The inverse of $\mathbf{C}$ can be factored:

$$\mathbf{C}^{-1} = \mathbf{W}\mathbf{W}^T \tag{3.24}$$

For the minimum norm, $\mathbf{W}$ is taken as the identity matrix $\mathbf{I}$. Taking $\mathbf{W}$ as the spatial Laplacian produces a spatially smooth solution, similarly to LORETA [Pascual-Marqui 94]. The α and β hyperparameters can be related to the λ presented in the previous section.

For more complex structures of the *a priori* probability functions, there may not be a simple analytic solution. An option is to compute values of the posterior probability for a large number of parameters values, representative of their range. This process is referred to as "sampling the posterior density", and can be accomplished by the Markov Chain Monte Carlo (MCMC) technique [Schmidt 99].

Statistical parametric maps

Some authors have attempted to construct maps that reflect the probability of having a source at a given point in the head, instead of producing only one "best" solution that could hide the existence of other likely solutions. This is actually an area of active research. These maps have sometimes been referred to as "Statistical Parametric Maps" (SPM), as a reminder of the similarity with the fMRI maps[1] [Friston 95]. As in fMRI, making inference on the statistical maps means handling a large multiple comparison problem.

One of the earliest contributions to this field was by Pedro Valdés-Sosa and colleagues. They proposed to use distributed sources methods (VARETA, [Valdés-Sosa 96]) to compute

[1]It is interesting to note that one of the reasons for choosing the name SPM was originally as a reference to "Significance Probability Mapping" in EEG.

at each point in the cortex the log power[2] of the time course of the sources, for each frequency bands. They computed a z score to evaluate the deviation at each point, given the frequency band and the age, from normal population data. They defined this procedure as "tomographic quantitative EEG" [Valdés-Sosa 97, Bosch-Bayard 01]. The significance of the scores were evaluated with the methods of Worsley [Worsley 96].

Similarly, Pascual-Marqui and colleagues have produced LORETA images of spontaneous (rest) EEG for both schizophrenic patients and control subjects. They computed the log-spectral power for different spectral bands, and computed t-tests at each voxel to assess the difference between controls and patients in each band [Pascual-Marqui 99]. They did not attempt to threshold the resulting images.

In [Dale 00], the energy of the sources amplitude in a distributed model were normalized by the energy of the noise, which is equivalent to having an F value at each point that tests for presence of activity. In [Pantazis 03], the distribution of such statistic under the null hypothesis was found with a non-parametric method that does not make any assumption on the shape of the distribution. Moreover, this permitted to handle the multiple comparison and to find a proper threshold for the images.

Barnes and Hillebrand have used a spatial filter (*beamformer*) in order to compute a t-test of power change at each given point in the head [Barnes 03]. They measured the smoothness of the image in order to correct for the multiple comparison problem.

Another line of research lies within the Bayesian formulation [Hämäläinen 88, Baillet 97], which is well suited as it is by essence probabilistic (and permits to include the linear distributed sources formulations as shown in the previous section). Clarke used this formulation and the concept of entropy, for the distributed model [Clarke 89, Clarke 94]; in [Hasson 99], the dipole model was used. Schmidt and colleagues have proposed the use of cortical patches of different location and extent [Schmidt 99]. The Bayesian framework allowed them to estimate the probability of the number, position and extent of sources.

3.3.3 Use of fMRI information

In the context of the ill-posed nature of the EEG inverse problem, the incorporation of spatial information from other modalities such as functional MRI seems an interesting option.

[2]The log transformation is useful to obtain a distribution of values that is more Gaussian.

The simplest way of combining information from EEG and fMRI is to perform the localization separately with the two modalities, and then compare them visually. Once some correspondence has been established between the regions detected in the two modalities, the order or amplitude of activation across regions can be inferred from EEG (see for example [Rossell 03] and [Toma 02]).

In order to push this approach one step further, several frameworks have been proposed to perform a more formal integration of EEG and fMRI results, which we will review here.

Dipolar models and fMRI

When considering dipole models, a first option is to force one dipole in each activated fMRI region and infer its time course of activation by fitting the amplitude only [Menon 97, Opitz 99].

One can use a regional source (or equivalently a rotating dipole) that explain all the dipolar activity in the region. The existence of EEG sources not detected by fMRI can be probed by adding other dipoles in the model, or performing source localization independently. In [Ahlfors 99], it is recommended to perform a localization step independently of the fMRI, and then use the fMRI information to refine the model

A pitfall is when there is a region active in fMRI but not visible with EEG. One would hope that including it in the EEG model will produce a fitted time course that resembles noise, but this is not guaranteed. Indeed, a very important consideration in the dipolar technique is that of "cross-talk" between dipoles. As the electrical field of neighbouring dipoles with similar orientations are very alike, enforcing a dipole in a region close to a true source will likely capture some of the signal produced by this latter. Indication of this effect can arise from two dipoles having very similar orientation and time course.

This approach is often referred to as "seeding" dipoles; this is somehow misleading. Indeed, traditional dipole modelling implies a non-linear optimization of the dipole location. In this context, a "seed" is an initial guess of the location, which is subsequently modified in order to improve the fit. This latter approach is actually to be considered in the situation of fMRI-guided modelling where one does not expect the best dipole model to be precisely at the centre of the fMRI activation, because of modelling errors, of the difference in nature of the measured quantities [Nunez 00] and of the fact that the dipolar model can lie deeper than the actual cortex. However, it is not guaranteed that the starting configuration is

stable in the minimization, for good reasons (wrong model) or bad reasons (there is another close local minimum, for example one ghost dipole in between two close real dipoles).

Forcing a dipole in a fMRI "hot-spot" at a small distance from real neuronal activity may not be too detrimental, though, as a dipole fitted at a short distance from the best-fit location should have a time course that resembles that of the best-fit dipole (there is at least something to be gained from ambiguity!).

The technique of spatial filtering (beamformer) is potentially very interesting in finding whether a region with fMRI activation contains an EEG source, while minimizing the influence of other (uncorrelated) EEG sources.

Weighted minimum norm and fMRI

The formulation (3.23) for the linear distributed sources allows for weighting differently the contribution of each source, simply by giving it a non-unity weight in the corresponding term in the diagonal of $\mathbf{C}$. This can been used to give more importance to the sources in the region of fMRI activation. Liu et al. verified that the EEG inverse solution was improved in regions with a corresponding fMRI activation, and that regions with an EEG source and no fMRI activation were still recovered [Liu 98]. Babiloni et al. investigated the optimal tuning of the value of the weight [Babiloni 00] and the influence of SNR and number of electrodes [Babiloni 03].

Bayesian framework and fMRI

The Bayesian formulation seems a natural way of integrating in the inverse problem all the *a priori* knowledge such as anatomical constraints, source waveform [Baillet 97], and of course fMRI activation.

In fact, the weighted minimum norm presented in the previous section can be derived within the Bayesian framework: the weights are the *a priori* probabilities of each source being activated. The off-diagonal terms in $\mathbf{C}$ can also be changed to reflect the joint probability of two sources being active together (Jérémie Mattout, personal communication).

The Havana group presented an innovative and somehow provocative framework, in which EEG and fMRI are considered in a symmetric manner [Trujillo-Barreto 01]. Within this approach, the two sets of data are processed together, and EEG can be seen as helping the fMRI localization just as much as the converse.

3.4 Precision of Source Localization Techniques

The sources of localization error are numerous: bias from the method, imprecision in head model, presence of spatially and temporally correlated noise, non-dipolarity of the sources, insufficient spatial sampling, etc...

Grave de Peralta-Menendez and Gonzalez-Andino proposed a theoretical framework for comparing the different methods. They considered the "resolution kernel", i.e. the capacity of a given method to resolve a point source [Grave 98b]. They also point out that linear inverse solutions can produce ghost sources, even in ideal noise-free situations [Grave 98a].

Baillet used a head physical phantom, i.e. a human skull filled with solidified gelatin, in which electrical dipoles were created by injecting a 2 μA current with a dipole length of 7 mm (equivalent dipole of 14 nA·m, with no noise) ([Baillet 98], see also [Baillet 01b]). For a spatio-temporal fit in a spherical head model, the localization error was of the order of 6 to 20 mm (mean 12.5). For the LORETA method, again in a spherical head model, the distance between the maximum of LORETA and the true dipole ranged from 20 to 40 mm (mean 26.8 mm). With both LORETA and dipole fit, a spurious deep source was found that was attributed to the spherical head approximation. Baillet simulated a cortical surface that contains the artificial dipoles, and used it as a constraint in the source estimate. In this context, the error for the minimum norm estimate ranged from 0 to 80 mm (mean 26.6 mm) in an anisotropic FEM head model. There were numerous small spurious detections along the cortical surface. He tested the ST-MAP method of Baillet and Garnero [Baillet 97], a distributed sources method that uses a potential function which takes into account the anatomy of the cortex in order to preserve intensity jumps, for example for dipoles situated on opposite walls of a sulcus. The results for the ST-MAP in the FEM model ranged from 0 to 15 mm (mean 0.25). They found similar mean results for FEM and spherical model, and proposed that in the spherical model "the loss of information regarding geometry and the fine conductivity parameters may be compensated by the resolution of the forward problem with the analytical formulation".

Knösche performed simulations and tests on somatosensory evoked potentials with both dipolar and distributed sources models [Knösche 97]. He found that the results of the two methods agreed well. He pointed out that in the case of close focal sources, such as those arising from median nerve stimulation, only the fixed sources model could disentangle them. This shows the interest of having less degrees of freedom, when the assumption

(focal sources) is fulfilled.

Krings et al. created artificial dipoles by injecting current between contacts of depth electrodes in several patients [Krings 99]. They performed dipole localization with a sherical head model, and found a mean error of 17 mm with 21 electrodes and 13 mm with 41 electrodes. The average signal to noise ratio (SNR) ranged between 4 and 6. Cuffin et al., with the same method, found an average dipole localization error of 9.1 ± 4.2 mm with a realistic head model [Cuffin 01a].

3.5 Clinical Relevance of Source Localization

Different groups have studied dipole models of epileptic spikes and seizures for patients with temporal lobe epilepsy ([Ebersole 90, Baumgartner 95, Boon 97, Merlet 96]; review in [Ebersole 97]). They found that the orientation of the dipoles could be used to distinguish sources in basal, tip or lateral neocortex. Moreover, they found that patients with hippocampal onset have a leading dipole in the basal region, that evolve into an oblique dipole suggesting basal and lateral involvement. On the contrary, patients with lateral temporal onset have spike and seizure dipoles oriented radially.

Scherg and colleagues have shown that a spatio-temporal dipole analysis could suggest patterns of propagation in both temporal and extra-temporal lobe epilepsy [Scherg 99]. They emphasized the importance of careful signal filtering, planning of analysis steps, and of including the initial component of the spike.

Spikes visible on the scalp reflect mainly superficial activity, but can include deep activity as well. Merlet and colleagues proved that EEG source localization can retrieve deep activity by averaging several spikes in order to improve the signal-to-noise ratio. They averaged spikes visible only in foramen ovale (intracranial) electrodes but not on the scalp, and verified that the equivalent dipole was in the mesio-limbic region [Merlet 98].

Several groups have used indirect methods for validating the results of dipole modelling in a clinical settings, by comparing them with post-operative results [Herrendorf 00], lesions [Boon 97] or metabolic findings [Merlet 96]; they generally found very good concordance.

In [Lantz 94], the dipole positions were compared with the ictal onset zone as determined by intracranial recordings (subdural or epidural) or intraoperative electro-corticography. They found that in 14 patients with a localized seizure onset (both temporal and extra-temporal) the dipoles were in good agreement with this region.

Merlet and Gotman compared the location of dipole models fitted on epileptic spikes to that of the intracerebral electrode of maximum activity. They found a mean distance of 11 ± 4.2 mm, with a spherical head model [Merlet 99].

Lantz and colleagues compared the results of LORETA with subdural recordings in seven patients [Lantz 97]. They found higher LORETA values in the area corresponding to the subdurally recorded spike compared to other areas.

Schwarz et al. demonstrated a good concordance between MEG dipoles location and order of timing with intracerebral recordings, except for deep mesial activity [Schwartz 03].

Santiago-Rodriguez and colleagues compared in 18 patients the results of dipole modelling and distributed sources (VARETA method), and found similar results for the two methods for 17 patients [Santiago 02].

3.6 Conclusion

The validation studies on artificial data show that the EEG source localization methods are capable in some conditions of retrieving the location of the sources with a precision of the order of 1-2 cm, and sometimes less in excellent conditions.

The clinical studies show that, in a real setting, the results of EEG source localization are concordant with direct or indirect estimates of the generators. Indeed, in the work of Merlet and Gotman [Merlet 99], the localization error is within the range of values obtained with simulations.

A critical issue is of course that of the validity of the modelling assumptions, that need to be carefully assessed, and the results must always be viewed in the light of these assumptions. It is not an easy task to assess which model is the most reasonable. Because of the high level of uncertainty, it is of interest to use any reasonable *a priori* knowledge, such as anatomical images (cf chapter 5), and to assess the range of possible solutions and their respective probability (cf chapter 8).

Chapter 4

Simultaneous EEG and fMRI

Functional MRI (fMRI) appeared in the beginning of the 1990's as a promising method for mapping brain functions non-invasively with very good spatial capacities. Only a few years after the advent of fMRI, it was proposed to record the EEG in the scanner concurrently with fMRI acquisition. This opened a whole new track for the study of spontaneous events such as epileptic spikes, which can only be seen with EEG during scanning. It is only several years later that EEG-fMRI started to spread, and it is currently an area of active research for spontaneous activity (e.g. alpha wave) but also for evoked activity. We will present in this chapter the bases of MRI, as well as the technique for acquiring and processing simultaneous EEG-fMRI data.

4.1 A Brief History of Magnetic Resonance Imaging

(Main source: [Raichle 98])

The links between neuronal activity and blood circulation started to be investigated at the end of the 19th century. Angelo Mosso (1846-1910) studied in 1881 the pulsation of the brain in patients with skull defects, and observed regional change with mental activity. Paul Broca (1824-1880) and Hans Berger (1873-1941) both noted an effect of mental activity on brain temperature. A seminal study in 1890 by Roy and Sherrington on animal models suggested a link between brain circulation and metabolism [Roy 90].

The team of Seymour Kety (1915-2000) was the first one to introduce quantitative techniques to measure animal brain blood flow, using autoradiography with a radioactive gas

as a tracer (1955). Later, Ingvar and Lassen in Scandinavia introduced scintillation detectors for measuring regional blood flow changes in humans (1963). Hounsfield introduced X-ray computed tomography in 1973, based on principles developed by Cormack in 1963. In the early 1970's, tomographic methods (back-projection) were also applied in Positron Emission Tomography, with the work of David Chesler at the MGH in Boston.

The principles of nuclear magnetic resonance were discovered in parallel by Felix Bloch and Edward Purcell in 1946, but were applied to medicine only in the beginning of the 1970's. The teams of Bloch and Purcell found that some types of atoms placed in a magnetic field and excited at a proper frequency absorb energy and re-emit it in the radio-frequency range. In 1950, E.L. Hahn presented the phenomenon of *spin echo*. In 1971, Raymond Damadian reported that cancerous tissue had different relaxation times to normal tissue. In 1973, Paul Lauterbur used a weak gradient magnetic field to create 2D images with back-projection. In 1975, Richard Ernst proposed to use phase and frequency encoding combined with the Fourier transform in order to generate images.

The road to functional MRI was opened by Ogawa and colleagues, when they reported changes in the MRI signal linked to local changes in blood oxygenation (which they called "Blood Oxygen Level Dependent" - or BOLD - effect) [Ogawa 92] . The first experiments were conducted with prolonged stimulation periods followed by rest (block design), as in PET. It was realized later that one could take advantage of the better temporal resolution of fMRI in order to study the response to brief events (event-related fMRI, [Josephs 97, Dale 97]).

4.2 Origin of the fMRI Signal

4.2.1 Physics of MRI

(Source: [Nishimura 96], [Pike 00])

A complete description of MR physics requires quantum mechanics; we will restrain ourselves to the more intuitive classical mechanics explanation. Magnetic resonance imaging is based on the fact that some nuclei (with an odd number of protons, neutrons, or both) possess an intrinsic magnetic moment. When placed in a strong magnetic field B_0, the individual magnetic moments align with the field and have a tendency to precess around it, like a top in the gravitational field of the earth. The frequency of precession ω_0 (resonance

frequency) is given by the Larmor formula: $\omega_0 = \gamma B_0$ (γ gyromagnetic ratio).

The individual moments align either parallel or anti-parallel to the longitudinal axis (along the direction of B_0), resulting in a net moment M_0 aligned with B_0. Now, if a field B_1 is briefly applied perpendicular to B_0 and at the resonant frequency, all the individual moments rotate around it. When B_1 is switched off, the moments return to equilibrium by precessing around B_0. The signal measured in MRI is the current induced by the net moment in a coil placed with its axis perpendicular to B_0. The amplitude of this signal is proportional to the number of atoms that have been excited by B_1.

The recovery of the equilibrium net moment M_0 along the longitudinal axis follows an exponential law with time constant T_1. Along the transverse axis (i.e. along the direction of B_1), the recovery is much faster, with constant T_2. Indeed, interactions between neighbouring moments cause random fluctuations in the precessing frequency and dephasing between individual moments, thereby reducing the net longitudinal moment (cf. Fig. 4.1). Different types of tissues have different time constants T_1 and T_2: this property is used to generate contrast between tissues in the resulting images.

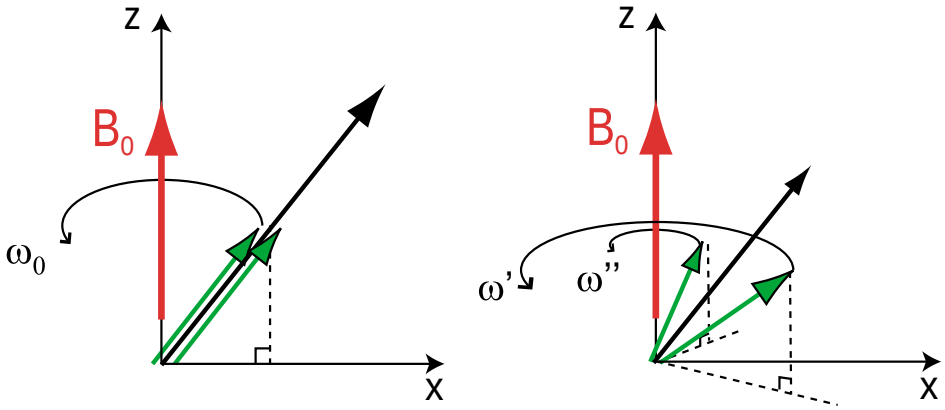

Fig. 4.1 Illustration of the effect of dephasing of two individual magnetic moments on the net moment. Left: The two moments (in green) precess at the same frequency $\omega_0 = \gamma B_0$. Right: Interaction with neighboring molecules produces dephasing after a short time; the component along the x-axis of the resulting moment (black vector) (transverse axis) - which generates the signal measured in MRI -is smaller than on the left.

In order to produce a 3D image, one needs to spatially encode the output signal. This is done with gradient fields, which introduce in turn variations in the main field proportional to the position along each axis. As the variations of the field induce differences in precessing

frequency, position is encoded in the resulting signal by frequency (i.e. the image is obtained in Fourier space). In echo-planar imaging (EPI, [Mansfield 77]), a whole slice is imaged after each excitation pulse, enabling a whole head scan in less than 3 s, which is very demanding in gradient switching speed.

Magnetic inhomogeneities in the medium cause further shortening of the transverse recovery time, resulting in a total time constant $T_2^* < T_2$. This is for example the case for deoxyhemoglobin (dHb), which is a by-product of brain activation (cf. next section).

4.2.2 The BOLD effect

The increase of metabolism in a neuronally activated area leads to an increase in oxygen extraction from the blood, and production of dHb. As there is concurrently a disproportionate increase in blood flow, the concentration of dHb decreases locally, and the MR signal increases [Hoge 99]. This is the Blood Oxygen Level Dependent (BOLD) effect [Ogawa 92], that takes places mainly at the level of the venous compartment (cf. Fig. 4.2). The BOLD response to a short stimulus is called the haemodynamic response (HR), which presents a main positive lobe followed by a negative undershoot, the whole phenomenon lasting around 30 s. The slow aspect of the HR is a limit in the temporal resolution of fMRI, even though time differences of the order of 100 milliseconds have been measured in particular conditions [Menon 98b].

Buxton et al. have presented a popular model for describing the mechanisms responsible for the BOLD effect, the Balloon model [Buxton 97, Buxton 98]. This model makes use of a venous "balloon" that receives the input of the capillaries and constitutes the main area of blood volume changes within the venous compartment. The apparent decoupling between a (small) change in oxygen consumption ($CMRO_2$) and a (larger) blood flow increase is explained by the passive properties of oxygen diffusion through capillaries. These workers argue that an increase in blood flow leaves less time for the diffusion of oxygen, therefore a disproportionately larger increase in flow is needed in order to have an increase in O_2 supply. Therefore, this model is in fact consistent with a tight coupling between $CMRO_2$ and blood flow. In [Buxton 98], the undershoot is explained by a slower return to baseline of the venous balloon volume compared to that of blood flow, which leads to a transient higher dHb concentration.

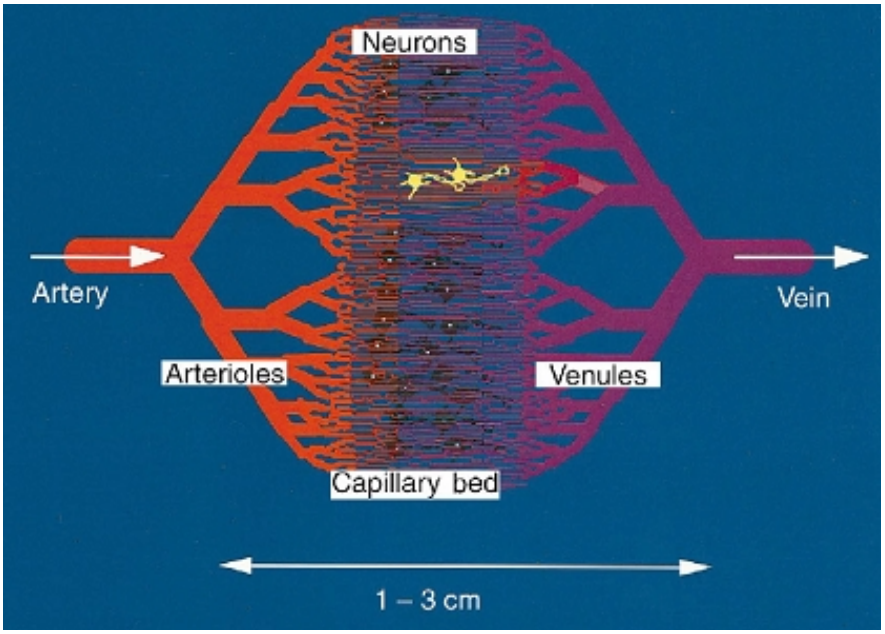

Fig. 4.2 Illustration of cerebral vessels. The activity of neurons results in a local increase of blood flow (From [Menon 99]).

4.3 The Technique of Simultaneous EEG-fMRI

4.3.1 Data acquisition

EEG recording in the scanner

The pioneer of concurrent EEG and fMRI recordings is John Ives in Boston [Ives 93]. This was an audacious move, as the MR scanner is obviously a very unfriendly place for EEG recording. Indeed, the machine generates continuously a large static magnetic field, and a rapidly changing magnetic field during the actual scanning period. Any movement of the electrode wires inside this large magnetic field or any variation of the field around a closed circuit induces currents that manifest as an artefact in the EEG [Ives 93]. Outside of the scanning period, subtle movements of the head or vibrations of the scanner can cause such artefacts. When the magnetic field is rapidly changing during scanning, a strong current is induced (gradient artefact) causing a distortion with an amplitude that can be of the order of 50 times the background EEG. Therefore, caution must be taken so as to reduce these effects, for the quality of the EEG but also for safety reasons [Lemieux 97, Lazeyras 01, Bonmassar 02].

The EEG electrodes and wires need to be non-magnetic; this is the case for the classical Ag/AgCl electrodes that are typically used clinically. Care must be taken as to avoid loops in the wires and minimize the surface area of closed circuits. It has been proposed to twist pairs of wires to achieve this goal [Goldman 00].

The faithful recording of the gradient artefact is an important condition of its eventual removal. It is crucial that the signal remain in the linear range of the amplifier, i.e. that the amplifier does not saturate. It has been reported that one may need a sampling frequency of 5 kHz so as to capture fully the shape of the gradient artefact [Allen 00], even though it is conceivable that strong analog anti-aliasing filters could allow lower sampling rates.

Typically, the amplifier is linked with a fibre optic cable to a computer located outside the MR room. The fibre optic is needed to ensure the absence of an electrically conductive bridge between the outside and the inside of the scanner room, a bridge that would deteriorate the quality of MR images.

EEG-triggered protocol

The first reports of combined EEG and fMRI recordings in epilepsy made use of a "spike-triggered" paradigm, where one image frame is acquired 3 or 4 s after each spike, taking advantage of the fact that the haemodynamic response peaks several seconds after the neuronal event [Warach 96, Seeck 98, Krakow 99]. An equivalent number of "baseline" frames has to be acquired. This approach does not require filtering of the gradient artefact because the EEG is visible between the brief scanning periods, but presents some drawbacks: only as many frames as spikes are acquired in total; low frequency drifts cannot be taken into account (see below); and an EEG specialist needs to be actively monitoring the recording during the whole session. It has been proposed to inject a short-acting anticonvulsant (Clonazepam) in order to obtain a long baseline completely free of spikes [Lazeyras 00]. This can be particularly interesting in the case of patients with a high spiking rate for whom it is difficult to obtain spike-free baseline sections. Such a baseline may be difficult to compare to the spiking section however, because of possible alterations of metabolism following the injection.

Continuous recording

The possibility of filtering the gradient artefact (see below) has opened the way for continuous recording of fMRI frames [Allen 00, Lemieux 01b]. In addition to not requiring constant monitoring of the EEG, this method permits to improve statistics by sampling a large number of points. It also allows calculation of the fMRI response to the spikes.

The range of spiking rates for which one can obtain a response is an open question. Too low a spiking rate may not allow for detection of activated areas, or to spurious detections because of the non-specificity of the resulting linear model. Too high a spiking rate is potentially problematic, as this could lead to a signal with few variations, or at least make the statistical detection rely heavily on the assumption of linearity (see section on statistical processing).

Image quality

Krakow et al. reported images (anatomical T1 and BOLD T2*) of good quality, despite the presence of electrodes and wires in the scanner [Krakow 00]. On the T1 images, some signal loss is visible around the electrodes; this is not detrimental, as it does not affect the brain. The fMRI T2*-weighted images are prone to having areas of signal loss in the basal frontal and basal temporal regions because of susceptibility artefacts [Ojemann 97]. This is problematic in epilepsy, as the basal temporal region contains structures often involved, such as the hippocampus and amygdala.

4.3.2 EEG processing

Gradient artefact filtering

Several groups have presented methods for removing the gradient artefact. A common approach consists in estimating the artefact and subtracting it from each frame. The first assumption is that the artefact and the background EEG add up, which is reasonable as currents are additive and care is taken that the amplifier stays within the linear range. The second assumption is that the shape of the artefact can be captured with sufficient precision. This means that the slope of the anti-aliasing filter must be steep enough to suppress the elevated power at high frequencies; this is rendered easier by a higher sampling rate. A marker signal can be collected from the scanner that indicates the start of each frame with

high precision. Allen et al. have used this marker to interpolate the signal of each frame to realign them before averaging [Allen 00]. Cohen et al. suggested triggering sampling on the marker, which removes the need to interpolate and renders the method more robust to aliasing [Cohen 01].

Generally, subtraction methods leave some remnants of the artefact; this is aggravated by the fact the artefact has much higher amplitude than the signal of interest. Allen et al. suggested using an adaptive filter based on the timing of each slice[Allen 00]. Anami et al. (2003) proposed an astute method where the signal is sampled at times with low artefact, in between gradients switching, which renders the task of filtering much easier [Anami 03].

Another option was that of by Hoffman et al. who took advantage of the frequency structure of the gradient artefact, i.e. a ray spectrum. A Fourier filter is constructed where the signal at frequencies with high power with respect to baseline EEG are zeroed [Hoffmann 00]. This approach is easy to implement and robust, in particular to movement artefact.

Pulse artefact

This artefact, also referred to as *ballistocardiogram* consists in small waves following each heartbeat. It possibly originates from small movements of the head or the electrodes following each pulsation because of fast movement of the blood in the arteries. It has been noticed from the first reports as one of the main problems when recording EEG in an MR scanner [Ives 93]. This artefact can be removed by subtraction [Allen 98].

4.3.3 fMRI processing

So far, the groups that have studied epileptic spikes with simultaneous EEG-fMRI have used classical fMRI analysis tools, which we shall briefly review here. However, one has to keep in mind that we are not dealing with a controlled paradigm, as in the typical stimulus-response pattern used widely in cognitive neuroscience. First, spikes occur at random. Second, they may be so closely spaced as to challenge the linear assumption made by most analyses of the fMRI signal: it is assumed that the BOLD effect of two spikes whose BOLD response overlap in time is the simple addition of the effects of the two spikes. Since the BOLD effect of a spike lasts 10 to 15 s [Lemieux 01b], this issue of linearity becomes relevant if spikes are separated by less than this duration [Buckner 98].

There is no evidence that the linearity assumption is correct in epilepsy. Third, spikes have different amplitudes, which are not necessarily correlated to that of the BOLD response. A possible reason is that the amplitude of spikes is more related to the extent of activated cortex than to the intensity of local neuronal activity. More generally, scalp EEG is only a very simplified reflection of what is happening within the brain.

Movement correction and smoothing

All MR images are very sensitive to movement, and this is a particularly important factor in long studies such as those required for obtaining a large enough number of spikes. It is possible to realign images with respect to a reference frame, for example the first frame of a series of frames.

Realigning the images is not sufficient for complete recovery of the fMRI signal though, as movement perturbs the sequence of alternate excitation/acquisition at a given slice. This was pointed out by Friston and colleagues, who advocated the use of the parameters of motion correction as additional regressors in the statistical analysis [Friston 96, Salek-Haddadi 03b].

Images are usually smoothed with a Gaussian filter with a full width at half maximum (FWHM) of the order of 8 mm, which helps reducing the noise in the BOLD responses when they involve more than one voxel. It also renders the analysis less sensitive to movements. It is possible that one could use a larger FWHM, as EEG epileptic spikes are expected to involve several cm^2 of cortex (cf. 2.2.3).

Statistical analysis

In event-related fMRI [Josephs 97], the statistical methods most widely used are probably those developed by Worsley and Friston [Friston 95, Worsley 95, Worsley 02]. In this "massive univariate" approach, the signal at each voxel is regressed on a model constructed by convolving impulses (corresponding to the timing of the spikes) with one or more basis functions. A statistical map (t-stat or F-stat, depending if one is testing for one parameter only or several at the same time) is constructed that reflects at each voxel the resemblance between the model and the data, and therefore the plausibility that this region is activated in response to the spikes.

The smallest basis function set consists in a standard haemodynamic response function

(HRF). This model assumes that each spike is followed by a stereotyped response, independent of the patient or the region. This is obviously a simplification, as it has been shown that even in a simple reaction time task, HRFs vary from subject to subject and even from session to session in a same subject, though to a lesser extent [Aguirre 98]. This approach will be challenged if the actual HRF differs too much from the standard HRF, or if the signal to noise ratio in the activated area is too low. Conversely, if the shape of the HRF used as a basis function is close to the actual response, then this is the approach with the best detection power (matched filter principle).

An option is to add the derivative of the HRF to capture small departures from an HRF standard model [Friston 98a]; the efficiency of this approach depends on the adequacy of the HRF model itself [Hopfinger 00, Della-Maggiore 02]. An interesting aspect of using a standard HRF only is that the resulting statistical maps are based on a t statistic, which permits to distinguish in a straightforward manner the positive responses (activations) from the negative responses (putative "deactivation").

Another common approach uses a set of basis functions, such as sines and cosines (Fourier set) or consecutive impulse functions ("finite impulse response", FIR). This has the advantage of allowing much larger variations in the shape of the actual response. The corresponding maps are based on an F statistic, which does not distinguish between positive and negative BOLD responses. With only a few activated voxels, one can verify the sign of the actual response at each voxel, but this becomes very tedious if the activated regions comprise a large number of voxels.

This statistical approach can be extended to include nonlinear effects [Friston 98b]. Also, techniques can be refined to capture the actual shape of the response, for example within the Bayesian framework [Marrelec 03].

Low-frequency drifts

Functional MRI signals typically present low-frequency variations, which possibly originate from scanner instability [Smith 99]. This drift can be modelled with a third-order polynomial [Worsley 02]. One could use a higher order polynomial; this would require investigation so as to find a good compromise between modelling the fluctuations and not removing parts of the signal. A possibility is to use a basis set of sine and cosine functions [Holmes 97]; this is similar to Fourier filtering, a method that potentially poses problems at

the boundaries and is prone to ringing artefacts. An engineering solution to this problem is to use a classical high-pass filter. It would then be necessary to take into account this filtering step in the effective degrees of freedom of the resulting data, which may not be as straightforward as with regressor-based filtering.

Thresholding

The first step in the interpretation of the statistical images is usually to apply a threshold of significance. The difficult problem of multiple testing has been elegantly answered by the work of Worsley using random field theory [Worsley 96]. One has to keep in mind that the HRF model and the linear assumption might not be optimal, resulting in reduced t values and possibly in missed responses. An interesting option is to use thresholds lower than the stringent single-voxel threshold, and take into account the number of connected voxels [Cao 99]. Poline and colleagues proposed a combination of single voxel and cluster thresholds, which aims at detecting both high intensity concentrated signals and widespread activity [Poline 97].

Aguirre, Zarahn and d'Esposito proposed to determine empirically the distribution of the statistics under the null hypothesis with the help of noise datasets [Zarahn 97, Aguirre 97]. They verified that the temporal correlation of the noise could be taken into account following Worsley and Friston [Worsley 95]. More recently, Worsley has proposed to prewhiten the data temporally, which has the advantage of increasing the number of degrees of freedom [Worsley 02].

4.4 Evaluation of fMRI Results

4.4.1 Brain versus vein

It is well known that functional MRI is prone to recording signals from large veins [Lai 93], particularly at 1.5 T. This could be particularly relevant in epilepsy, as epileptic spikes are assumed to involve large areas of cortex: the BOLD effect could be visible in draining veins relatively far from the site of neuronal activity. Following the calculations of [Turner 02], a neural activated area of 6 cm^2 could lead to a BOLD signal change at a distance of approximately 10 mm from the region of neuronal activation.

At higher field (3 T and more), the signal obtained from the capillaries is increased

because of a higher signal to noise ratio [Krasnow 03] (small veins are approximately less than 50 μm diameter). An interesting point is that the signal from larger veins does not increase as much [Gati 97]. Postprocessing has been proposed to remove the contribution from large veins (with diameter up to 0.5 mm) [Menon 02].

4.4.2 Link of fMRI with electrophysiology

The "activity" in a given region of the brain is usually conceptualized as the spiking rate of its neuronal population. However, it has been estimated some time ago that re-establishment of membrane potential after synaptic activity is more energy consuming than actual spiking ([Creutzfeldt 75], discussed in [Mathiesen 98]). This is an interesting question for the comparison of EEG and fMRI, as the former is thought to be the reflection mainly of slow membrane potentials rather than fast action potentials that are less likely to summate temporally [Speckmann 99].

Mathiesen et al. have shown on extracellular recordings in rat cerebellar cortex that both synaptic activity and spikes may contribute to the increase of blood flow [Mathiesen 98]. They stated that "it is impossible on the basis of an increase in regional activity to decide whether the spike activity in this region is inhibited or increased". Logothetis and colleagues have performed simultaneous microelectrode and fMRI recordings in the monkey, and separated the signal in two frequency bands, that of the local field potential (LFP, slow activity) and the multi unit spiking activity (MUA). They found that the LFP was a better predictor of the BOLD response than the MUA [Logothetis 01].

The link between energy demand and blood flow increase may be mediated in a large proportion by astrocytes that possess some processes close to the synapses on one hand and others surrounding capillaries on the other hand (cf. review Heeger and Rees [Heeger 02]). The link could be accomplished through nitric oxide, a vasodilator. The disproportionate increase in blood flow compared to oxygen consumption could be needed because of the low diffusibility of oxygen through the capillary walls (Buxton and Frank [Buxton 97], review by Hoge and Pike [Hoge 01]).

The linearity of the system linking neuronal activity and fMRI BOLD has raised much interest. It has been shown that in a range of duration of stimulation, the system was reacting quite linearly (3 to 24 s in [Boynton 96], 1 to 3 s in [Dale 97]). However, for short duration signals, the amplitude of the bold signal can be larger than predicted by a linear

system [Boynton 96]. This could be originating from a transient high neuronal activity at the beginning of the stimulation (in the form of action potentials), that would be consistent with the LFP recordings [Logothetis 01], as pointed out in [Bandettini 01].

Recently, Huettel et al. have investigated the relation between visual ERPs measured intracranially (subdural electrodes) and the BOLD response. They manipulated the duration of stimulation, and found different linkage between ERPs and BOLD reactions across regions [Huettel 04].

In terms of localization, optical imaging experiments have shown that the initial change in deoxyhemoglobin can be highly colocalized with the neuronal activity (first 3 s), but that its spreads over a distance of 3 to 5 mm in a later phase (Malonek and Grinwald [Malonek 96]). The fMRI signal is at 1.5 T is unlikely to be able to make a distinction between these two phases. Disbrow et al. have compared maps based on both fMRI and microelectrode recordings and have found a 55 % concordance (i.e. centroids of fMRI located in the electrophysiological map) [Disbrow 00]. In the unmatched cases, the mean error was of the order of 1 cm. This is consistent with the fact that large draining veins that may be located several mm away from the site of activation can make a significant contribution to the BOLD effect (cf. 4.4.1 and review [Menon 98a]).

Grimm et al. have performed 64-channels EEG source localization and fMRI studies using the same median nerve stimulation paradigm [Grimm 98]. EEG and fMRI resuts were always found within the postcentral gyrus. Only two subjects out of six had significant results for both modalities; their difference in localization was 5.1 and 11.9 mm.

4.5 Clinical Relevance of fMRI in epilepsy

4.5.1 Presurgical mapping

During surgical intervention, it is desirable to avoid resection of parts of the cortex that would lead to functional deficit. Direct electric stimulation of the cortex has been used from the start of epilepsy surgery in order to map the “eloquent” cortex, for example motor areas. This can be done also with chronically implanted electrodes. Intracarotid amobarbital injection, where one hemisphere only is anaesthetized, is a traditional means for lateralizing the language areas. Functional MRI can perform such localization non-invasively, and its use in presurgical planning is becoming more and more important (reviews in

[Vingerhoets 04] and [Richardson 03]).

4.5.2 Localization of irritative zone

The clinical value of simultaneous EEG-fMRI in localizing the sources of epileptic discharges is in the process of being established. Several groups have presented limited series of patients with good correspondence between fMRI and EEG or other sources of information (structural MRI, intracerebral recordings, surgical outcome).

We are reviewing here some of the work of the main groups that have reported series of patients. For a more complete list of articles, see [Salek-Haddadi 03a].

Boston group

The first case report of EEG triggered fMRI for epileptic patients was by Warach and colleagues, for two cases [Warach 96]. For the first case, with EEG suggesting left temporal localization, they found bitemporal activation. For the second case, there was no focal EEG findings, and a focus of increased signal in the anterior cingulate region.

Patel et al. have reported a series of 20 patients, 18 of whom had spikes during a 1- to 2-hour recording [Patel 99]. They performed manual triggering of image acquisition with visual assessment (EEG-triggered method); the imaging time ranged from 1 % to 50 % of the time in the scanner depending on spike frequency. They rejected three patients because of a high level of motion. They performed three types of analysis: subtraction spike versus baseline, correlation analysis and single spike analysis. For the single spike analysis, they evaluated the presence of "bright areas"; they found regions consistent with the EEG discharge in 9 patients out of the 10 for whom the analysis was performed. They also computed a z-score for the activated areas; they present two examples with highest scores of 2.9 and 3.6.

Geneva group

Seeck et al. described in [Seeck 98] their method of comparing EEG-triggered fMRI and EEG 3D source localization. They present the results for one patient with frontal lobe epilepsy, for whom no lesion had been found. One image frame was acquired after each spike was noted. Two series of 60 frames were acquired after injection of Clonazepam in order to get a spike-free baseline. A statistical map was computed by a cross-correlation

analysis, and a threshold corresponding to p=0.005 (uncorrected) was used. Only the clusters with more than 10 voxels above the threshold were considered.

They found three clusters, one left frontal, one in the interhemispheric area, and one right frontal. The LORETA method pointed to the same three regions, and enabled them to follow a propagation from left to right. The inspection of MRI, which had previously been reported as normal, revealed an area of thickened cortex concordant with the left cluster. The patient was operated, and subdural recordings confirmed the involvement of the left region. Only partial resection of the left region was performed because of an overlap with speech functions. After operation, a follow-up of six months showed a marked reduction in the number of seizures (5 in six month versus 5-12/week).

Later, Lazeyras et al. reported the results of spike-triggered recordings in a group of 11 patients with pharmacoresistant epilepsy [Lazeyras 00] (including the case report of [Seeck 98]). The regions of activation were found by cross-correlation with a step function. A Bonferroni correction was used to assess statistical significance, and only clusters of 10 voxels or more were considered. In 7 patients (64 %), focal regions of signal enhancement were found, that were always consistent with other sources of information (EEG, imaging, invasive recordings). For two patients, images are shown that compare the focal areas of activation with results from subdural and depth electrodes recordings. There is no exact overlap of intracranial EEG and fMRI results, but there is a good correspondence at the level of the cm.

London group

Krakow and colleagues [Krakow 99] reported a series of 10 patients, with a total of 24 recording sessions (2 to 4 per patient). Five patients had activations in all sessions (2 to 4 sessions), one patient in 2 out of 3 sessions only, and one patient in 1 out of 2 sessions. All the areas of activation were concordant with EEG or lesional findings. In one case, localization in the left superior temporal lobe was confirmed with electrocorticography. In three cases, the side of fMRI findings were concordant with ictal EEG lateralization. In three patients with focal lesions (hippocampal sclerosis, cortical dysgenesis, tumour), the activations were overlapping or adjacent to the lesion. In two patients of the series, the authors found that the fMRI was more sensitive to the area of primary spike generation than the propagated areas. For the three patients with no activation (30 %), the authors

postulated that it could be related to the fact they had EEG activity of lower amplitude.

The same group reported in [Krakow 01] a series of 24 patients (that includes those of [Krakow 99]). Twelve patients (50 %) presented an fMRI activation that was consistent with EEG findings, and with MR abnormality when present (7 out of 12). In two patients, fMRI activation was non-concordant with EEG findings. In the remaining 10 patients, there was no significant activation.

Lemieux et al. performed source localization on epileptic spikes with 64 channels and EEG-triggered fMRI on separate sessions for a group of six patients [Lemieux 01a]. They found a mean difference of localization of 3.5 and 2.2 cm for the negative and positive peaks of the spike respectively. For one patient with a deep BOLD activation, the distance was 5 cm.

4.5.3 Ictal fMRI

In uncontrolled conditions, one typically would not want a patient to have a seizure within the MR scanner, first of all for safety reasons. Another drawback of ictal fMRI is induced movements, as fMRI is very sensitive to even small movements of the head. Nevertheless, several reports have been made of successful recordings of subclinical seizures (i.e. with no clinical manifestation) or seizures with only little movement.

In 1994, Jackson (who was at the time at the Institute for Child Health in London) and colleagues published a case study of a 4 year old boy with putative Rasmussen's encephalitis[1] [Jackson 94]. The patient was sedated, and seizures were noted by visual observation. One slice was recorded (FLASH sequence [Frahm 86]) every second, which included the area of maximum MRI abnormality. Activation images were obtained by subtracting baseline data from seizure data. Areas of high intensity were found that were consistent with SPECT and structural abnormality. They tracked the temporal course of the fMRI signal in regions of interests, and found that signal increased just before the seizures.

In a study by Detre et al, there was no seizure reported during the fMRI experiment, but areas of high signal changes were found that were consistent with subdural recordings [Detre 95]. Krings et al. reported a case where one partial seizure took place in the

[1] Rasmussen encephalitis is a chronic, progressive inflammation of the brain of unknown origin. The onset is in childhood and is characterized by an abrupt appearance of focal, persistent motor seizure activity, followed by hemiplegia and progressive cognitive deterioration (citation adapted from foundation.asnr.org)

scanner (Jacksonian march involving left foot then leg) [Krings 00]. Large signal changes were noted around the time of the seizure, that suggested a clear sequence of propagation. In particular, changes were noted in the perilesional area, with no change in the foot area, 65 s before the clinical signs.

Salek-Haddadi and colleagues have performed recently an ictal study with simultaneous EEG-fMRI, that enabled them to analyze data related to a subclinical seizure visible on EEG [Salek-Haddadi 02]. They computed a statistical map, taking into account the parameters from motion correction in order to take into account movement-related signal changes [Friston 96]. They found a large area of activation concordant with the location of EEG activity. They also reported a case with absence seizures, where thalamic activation and widespread cortical deactivation were seen [Salek-Haddadi 03b], consistent with current hypotheses on this type of seizures.

The reflex epilepsies, in which seizures can be induced by certain stereotyped stimuli, are good candidates for ictal fMRI studies. Such studies have been reported for musicogenic [Morocz 03] and reading epilepsy [Archer 03b].

Opdam et al. in Victoria have introduced a sheep model for fMRI ictal studies. They induced seizures by applying penicillin, and recorded intracranial EEG with carbon fibre depth electrodes [Opdam 02]. The animals were anaesthetized during the fMRI experiment. They observed fMRI changes both at the site of injection and the amygdala.

4.6 Conclusion

BOLD fMRI is a complex technique that depends on a cascade of physiological phenomena, as well as advanced considerations in physics and statistical processing. The simultaneous recording of EEG and fMRI in epilepsy adds two sources of potential problems. One is the recording of the EEG inside the scanner and the post-processing of the resulting data. The other is the fact that the epileptic activity cannot be controlled as in event-related paradigms, and that we only have a poor reflection of this spontaneous activity in the form of scalp EEG.

In spite of these problems, very encouraging results have been produced in EEG-fMRI studies of epileptic patients, and the technique is likely on its way for clinical use. In chapters 6 and 7, we will present two aspects of simultaneous EEG-fMRI: the EEG recorded in the scanner on the one hand and the fMRI results, both in terms of temporal and spatial

response, on the other hand.